

Spring 2010

Development of a functional MRI Olfactory Protocol

Jeremy Mangum

University of Nevada Las Vegas

Follow this and additional works at: <https://digitalscholarship.unlv.edu/thesesdissertations>



Part of the [Neurosciences Commons](#), and the [Radiology Commons](#)

Repository Citation

Mangum, Jeremy, "Development of a functional MRI Olfactory Protocol" (2010). *UNLV Theses, Dissertations, Professional Papers, and Capstones*. 11.

<http://dx.doi.org/10.34870/1343134>

This Thesis is protected by copyright and/or related rights. It has been brought to you by Digital Scholarship@UNLV with permission from the rights-holder(s). You are free to use this Thesis in any way that is permitted by the copyright and related rights legislation that applies to your use. For other uses you need to obtain permission from the rights-holder(s) directly, unless additional rights are indicated by a Creative Commons license in the record and/or on the work itself.

This Thesis has been accepted for inclusion in UNLV Theses, Dissertations, Professional Papers, and Capstones by an authorized administrator of Digital Scholarship@UNLV. For more information, please contact digitalscholarship@unlv.edu.

DEVELOPMENT OF A FUNCTIONAL MRI OLFACTORY PROTOCOL

by

Jeremy Mangum

Bachelor of Science
University of Nevada, Las Vegas
2004

A thesis submitted in partial fulfillment of
the requirements for the

Master of Science in Health Physics
Department of Health Physics and Diagnostic Sciences
School of Allied Health Sciences
Division of Health Sciences

Graduate College
University of Nevada, Las Vegas
May 2010

Copyright by Jeremy Mangum 2010
All Rights Reserved



THE GRADUATE COLLEGE

We recommend the thesis prepared under our supervision by

Jeremy Mangum

entitled

Development of a Functional MRI Olfactory Protocol

be accepted in partial fulfillment of the requirements for the degree of

Master of Science in Health Physics

Health Physics and Diagnostic Sciences

Phillip Patton, Committee Chair

Steen Madsen, Committee Member

Ralf Sudowe, Committee Member

Merrill Landers, Graduate Faculty Representative

Ronald Smith, Ph. D., Vice President for Research and Graduate Studies
and Dean of the Graduate College

May 2010

ABSTRACT

Development of a Functional MRI Olfactory Protocol

by

Jeremy Mangum

Dr. Phillip W Patton Examination Committee Chair
Associate Professor of Health Physics and Diagnostic Sciences
University of Nevada, Las Vegas

Many people can spend a few days with an acute form of sinusitis, a stuffy nose, or sinus congestion that inhibits their ability to smell, but there are fourteen million Americans over the age of fifty that suffer from some form of chronic olfactory dysfunction. Some neurological disorders such as Parkinson's disease and Alzheimer's disease have demonstrated that olfactory dysfunction is a frequent and early sign. While these diseases have no known cure, there are medicines that exist to slow the progression of such debilitating illnesses. By identifying such diseases in their early stages, we can improve the quality of life for millions of people throughout the world.

This research project will begin to open the doors for more investigation into the relationship of olfaction and Parkinson's disease, Alzheimer's disease, and even epilepsy by the development of an fMRI olfactory stimulation protocol. This protocol successfully identified the olfactory regions of the brain of normal patients.

Keywords: functional MRI, olfactory, BOLD imaging

TABLE OF CONTENTS

ABSTRACT	iii
LIST OF FIGURES	v
CHAPTER 1 INTRODUCTION	1
The Olfactory Process	3
Physics of MRI and fMRI.....	8
CHAPTER 2 MATERIALS AND METHODS	16
Delivery Device Development.....	18
Image Acquisition.....	25
Image Processing	29
CHAPTER 3 RESULTS	31
Delivery Device and Set-up.....	31
Data Acquisition and Processing	35
Response to Different Scents.....	38
Factors Involving Image Acquisition.....	41
Factors Involving Image Quality	43
Image Data Results	48
CHAPTER 4 DISCUSSION AND CONCLUSIONS	52
Delivery Device	52
Data Acquisition	53
Data Processing.....	55
Different Scent Responses	56
Conclusion	57
REFERENCES	59
APPENDICES	64
A. fMRI Acquisition Method With Philips Intera and IViewBold Software	65
B. fMRI Processing Methods With Philips BrainVoyager 2.6.....	69
C. Patient Consent Forms and IRB Approval.....	76
D. Permission to Use Images.....	80
VITA.....	81

LIST OF FIGURES

Figure 1.1	Olfactory receptor neuron	5
Figure 1.2	The Limbic System (a modified Frank Netter Image)	7
Figure 2.1	Philips Medical System’s 3-T MR scanner used for acquisitions	17
Figure 2.2	Delivery mask.	18
Figure 2.3	Scent-containing boxes for delivery to patient.	19
Figure 2.4	Control valve with charcoal filter for oxygen administration.....	20
Figure 2.5	Complete diagram of olfactory delivery set-up	21
Figure 2.6	Bite-plate delivery device	22
Figure 2.7	Delivery device to be used with strap-on elastic	23
Figure 2.8	Coil-mounted delivery device (ultimately used for protocol).....	24
Figure 2.9	The design concept for a coil-mounted delivery device	24
Figure 2.10	Three-command form of dynamic block acquisition	27
Figure 3.1	Signal-response graph.....	32
Figure 3.2	Minimal activation seen on anatomical data set.	33
Figure 3.3	Signal-time course graph showing eye activated region.....	34
Figure 3.4	Increased activation in the early-stages of an acquisition with a prolonged “on” phase.....	36
Figure 3.5	Decreased activation in the late-stages of an acquisition with a prolonged “on” phase.	37
Figure 3.6	An example of a 64 dynamic, 3-phase, and acquisition block parameter.	38
Figure 3.7	Brain activated region of the thalamus due to alcohol inhalation.....	39
Figure 3.8	Brain activation as a response to inhalation of tabasco sauce	40
Figure 3.9	Activated brain regions with associated signal versus time curve.....	42
Figure 3.10	Field distortion due to metal retainer on lower jaw	43
Figure 3.11	wrap around artifact due to increased eddy currents	44
Figure 3.12	Motion correction scheme, showing alterations in 6 directions	45
Figure 3.13	Time-course plot with regional activation sites	46
Figure 3.14	Statistical data as received from GLM analysis.....	47
Figure 3.15	Coregistered image of functional data overlaid on anatomical data.....	48
Figure 3.16	Consistencies in functional imaging	50
Figure 3.17	Inconsistencies in functional imaging.....	50

CHAPTER 1

INTRODUCTION

For years the brain has been imaged through different modalities to analyze structure, size, shape, and function. The most recent, brain function, has advanced further than any other in recent years. Scientists and researchers alike are constantly trying to understand how and where the brain is able to comprehend and process information from different stimuli. By identifying what areas of the brain are activated for a given stimulus, we may better understand how the mind works. We will also be able to better determine the brain's functional capabilities following neurosurgery, therapeutic treatments, or traumatic events.

The olfactory system is currently a focused area of study in medical imaging, and the subject to which most of my research is focused. In 2004 the Nobel Prize in Physiology or Medicine was given to Drs. Richard Axel and Linda Buck, for their discoveries of odorant receptors and the organization of the olfactory system (Nobel Prize 2007). Their research opened the eyes of science to a bigger world of olfactory stimulation and processing (Shepherd 2006). It gave better explanations as to how and why we smell, especially explaining such concepts on the microcellular level.

Sniffing something is a way to enhance a scent or better identify what it is one smells. Air entering the nasal cavity stimulates olfactory receptors which in turn send signals to the brain (Marieb 2001). Research shows that we all have similar areas of detection in the brain, yet receptor sites vary from person to person (Machielsen et al. 2000; Schafer et al. 2006; Weismann et al. 2006). This creates difficulties when trying to image and compare areas of olfaction with fMRI against other subjects.

Neurological function as a response to stimulus involves a complicated process that is only beginning to be understood. With the advent of functional magnetic resonance imaging (fMRI), more and more information is being made available. The background ideas for what is known today as fMRI dates back to the late 19th century. The concept that neuronal activity is reflected from the regional cerebral blood flow (CBF) came about from experiments done in 1890 by Roy and Sherrington (1890). Their discoveries helped to show, what came to be the basis for all hemodynamic-based brain imaging, that neuronal activity can be related directly to the increases in CBF (Faro 2006). The ability that we have to image brain function with magnetic resonance imaging (MRI) relies on the ability to detect changes in deoxyhemoglobin (dHb) concentrations in the brain. These changes make it possible to implement a naturally produced contrast to enhance MRI images. This contrast is the venous blood oxygenation level-dependent (BOLD) contrast (Price et al. 2002). It relies on the changes in dHb concentrations to augment neuronal activity (Faro 2006). Applying this concept with the ability of standard MRI to distinguish cerebral regions, we are able to increase our knowledge of how and where the brain processes information from various stimuli.

Along with the aforementioned work, researchers have shown that fMRI is useful in measuring the functionality of various regions of the brain, but to what extent in olfaction is yet to be fully understood. Previous research has focused on other senses, such as the visual and auditory (Kamitani 2005; Liu 2005; Gomot 2006). Very little research exists on the repeatability and quantification of olfactory response. Due to multiple factors affecting the sense of smell, the olfactory process is one of the most

complex senses in our bodies. We have seen differences in the Limbic systems (where the olfaction structures are located) of male and female (Garcia-Falgueras et al. 2006). Tests have been done to see if reading the names of odors or scents will stimulate the desired sites (Gonzalez et al. 2006). Imaging patients with their eyes open versus eyes closed gives different responses for olfactory and gustatory processes (Weismann et al. 2006).

One of the biggest areas of olfactory research involves those who suffer from neurological disorders. Early detection of olfactory dysfunction can be a sign of neurological disorders such as Alzheimer's (AD) and Parkinson's disease (PD) (Huttenbrink 1995; Mueller et al. 2005; Bohnen et al. 2007; Tolosa et al. 2006). An early sign of AD and PD is one losing the ability to smell or recognize scents. These discoveries along with the idea that some smells may actually aid in stopping seizures have been an area of research for years (Whitfield and Stoddard 1984). Work has also been done to see how olfactory areas are affected by severe head trauma (De Kruijk et al. 2003; Green et al. 2003). Knowing that smell and taste are related, some researchers have been studying relationships between these internal activation areas and the olfactory and trigeminal nerves (Rozin 1982; Shepherd 2006; Iannilli et al. 2007). Much of the repeatability studies have been done with rats, while those done on humans typically compared one person to another.

The Olfactory Process

Smell, also called olfaction, is the detection and identification by sensory organs of airborne chemicals (Encyclopedia Britannica 2007). This detection process originates

in the olfactory epithelium found in the roof of the nasal cavity. In order to be detected, the substance must be in a gaseous form and soluble in water upon entering the nasal cavity. The solubility is important in the odor reception process, because the olfactory epithelium is coated with a fluid or mucus (Shepherd 2006). This layer of mucus is the medium where odor molecules, odorants, are dissolved. Once dissolved, they bind to an odorant binding protein, OBP, which are thought to facilitate the transfer of odorants to the receptor (Jacob 2007). Once broken down in the mucosa, the molecules travel through the epithelium, through the cribriform plate, and into the cerebrum where it follows the path of the olfactory tract. Located in the mucosa of the olfactory epithelium are tiny cilia. These cilia interact with the odorant molecules and begin the transmission processes for detection. Cilia are actually the end fibers of the olfactory receptor neurons. Each neuron has 8-20 cilia, all of which range in length from 30 to 200 microns (Leffingwell 1999). The olfactory receptor neurons are located in the base epithelial layer. At the other end of these neurons are found the axons. The axons leave the epithelium and extend through the cribriform plate and into contact with the olfactory bulbs. The axons converge and combine with cells to form glomeruli. Multiple glomeruli then converge into mitral cells. Figure 1.1 shows a representation of an olfactory receptor neuron located within the basal cell with cilia dipping into the olfactory mucus. This convergence increases the sensitivity of the information that is sent to the brain for processing. Odor or smell information is sent from the olfactory bulb to the amygdala via the olfactory nerve tracts. Information is then processed and interpreted by the brain. The olfactory nerve can be considered the nerve of smell. Cranial nerve #1, CN1, the olfactory nerve, is one of only two nerves not arising from the

brainstem, the other being the optic nerve, or cranial nerve #2, CN2 (Crimando 2004). CN1 is actually the unification of small nerve bundles from the axons of the olfactory neurosensory cells. The olfactory nerve consists of small bundles, called fila; it is these bundles that pass through the cribriform plate of the ethmoid bone and end in the olfactory bulb (Voron 2006).

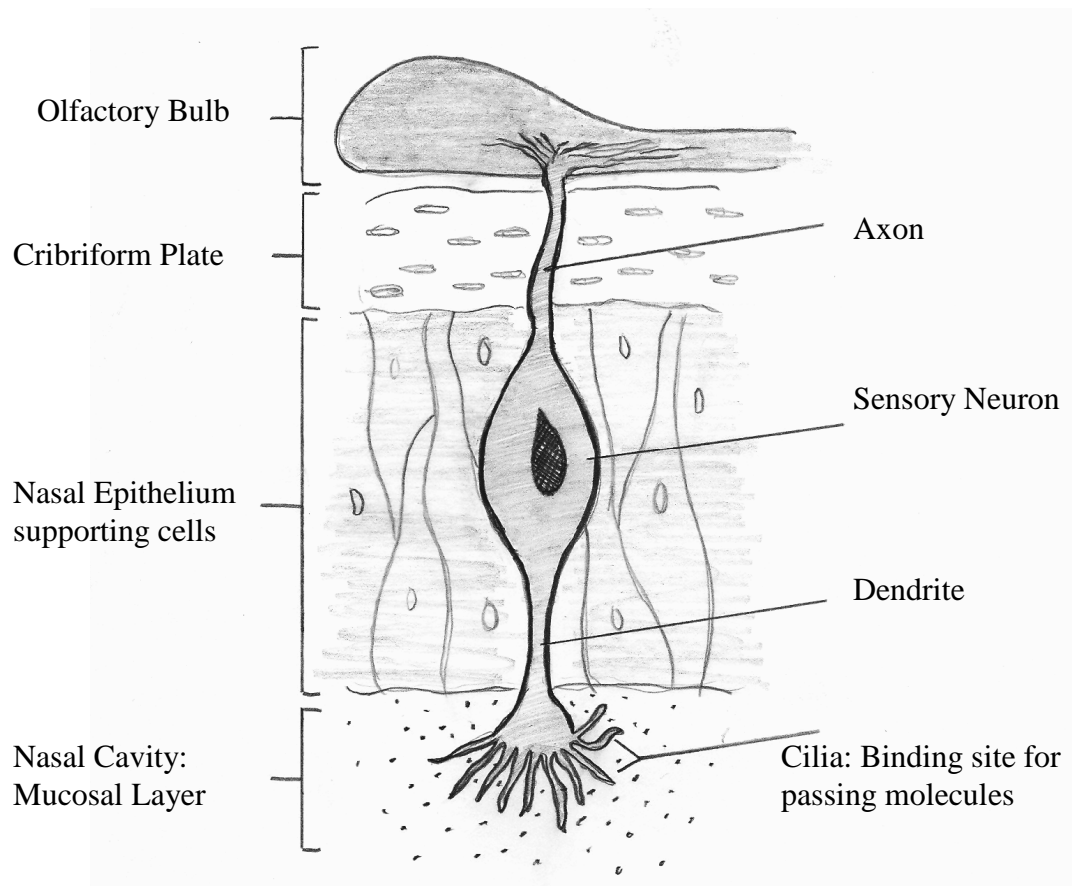


Figure 1.1. Olfactory receptor neuron.

The olfactory epithelium also contains nerve endings from the trigeminal nerve. The trigeminal nerve is the largest cranial nerve and is responsible for pressure, pain, and

temperature sensations in the mouth, eyes, and nasal cavities. Upon smelling some scents we may respond by saying that the smell was hot, cold, caused tingling, or even gave a sense of irritation. These responses are due to the interactions with the odorant chemicals and the trigeminal nerve endings, which detect caustic chemicals such as ammonia (Vokshoor 2006). Because of such interactions, various “non-smell” related areas of the brain may respond in functional neuroanatomical studies.

Imaging of the olfactory stimulated regions may also be more complicated when considering that there exists a dual form or origin of odorant molecules. This means that our ability to smell is not solely based on the odors entering through the nostrils of the nasal cavities. Scents that enter by way of our mouths through the food we eat or liquids we drink also have a way of stimulating our olfactory receptor neurons. These two origins have been referred to as orthonasal and retronasal stimulation (Rozin 1982; Shepherd 2006). Orthonasal stimulation is through the process of sniffing and stimulating the cilia of the epithelium. This is how we perceive odors in the environment. Retronasal stimulation occurs when we are eating food. Certain volatile, gaseous, molecules from the food are circulated up the nasopharyngeal region as we chew and breathe in the mastication process. Retronasal stimulation therefore originates in the back of the oral cavity and not in the exterior environment. This is where much of our sense of flavor recognition originates. Thus a large part of flavor is actually due to smell, or olfactory recognition. The retronasal process is not the same as the sense of taste. It is merely another way to describe the origination of volatile molecules that pass through the nasal cavity. Taste is the sensation produced by a stimulus applied to the gustatory nerve endings in the tongue (Children’s HL 2007).

The brain's ability to smell is very complex and also difficult to research. Any given odor can contain hundreds of different chemicals. Humans are able to distinguish an average of 10,000 chemicals (Marieb 2001). The olfactory system does not just identify smells; it also regulates a wide range of multiple functions such as physiological regulation, emotional response, reproductive functions, and social behaviors (Lledo 2005). This is in part due to the localization of the olfactory tracts, see Fig. 1.2. They incorporate themselves with the limbic system, which is known to be involved with aggression, sexual behavior, memory, learning, and emotional responses in general.

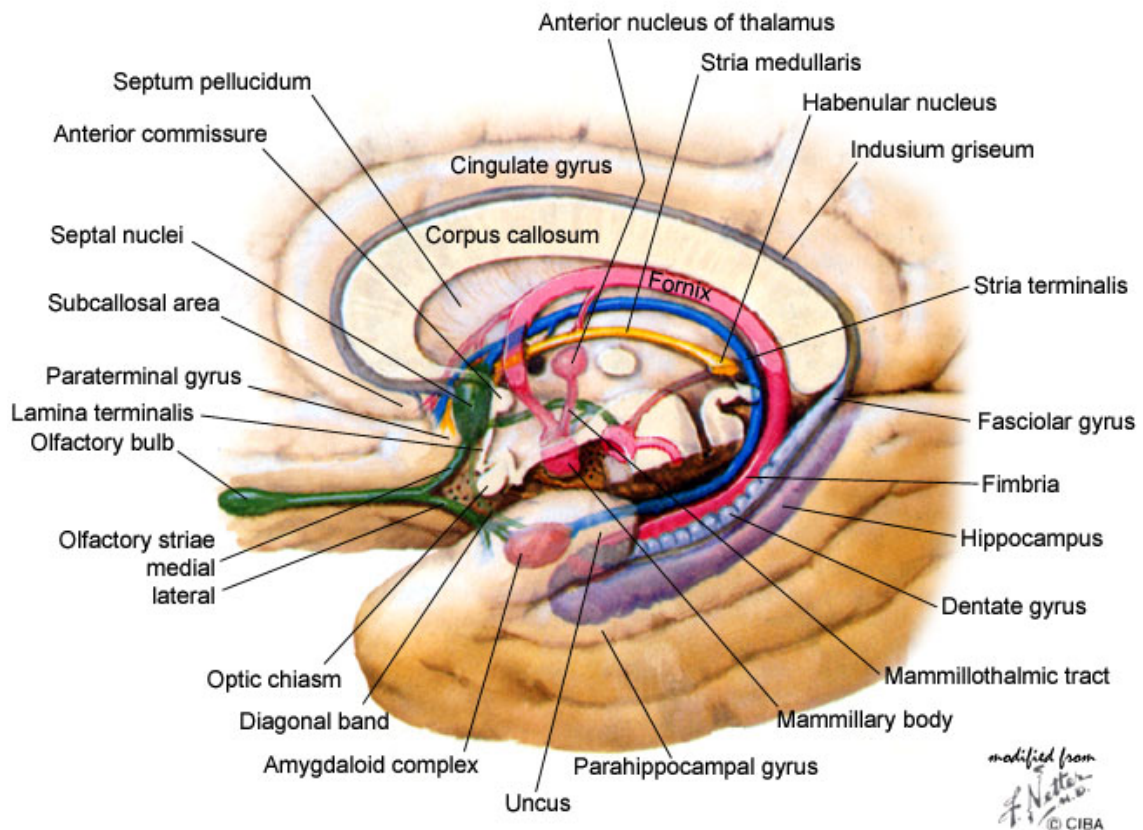


Figure 1.2. The Limbic system (Glowniak 2007).

The olfactory tracts pass underneath the frontal lobe and connect to a structure called the amygdala to bring information on the sense of smell to the limbic system. The amygdala is a mass of gray matter in the anterior medial portion of the temporal lobe and is partly concerned with olfactory reflexes and aggressive or sexual behavior.

The idea that the olfactory system is connected to the amygdala, which has a correlation with sexual behavior, also leads to questions relating to the understanding of male versus female results in olfactory testing. It has been shown that the olfactory system is indeed a sexually dimorphic system (Garcia-Falgueras 2006). This system is anatomically different between the two sexes and may therefore pose a theory that they may also be physiologically different.

Physics of MRI / fMRI

Detecting and analyzing magnetic signals has been studied extensively since the 1940's to further medical and physiological advancements (Bushberg 2002). Magnetic imaging does not involve ionizing radiation. Magnetic properties result from the motion of electrons in matter. Molecules and atoms contain electrons that are positioned in orbitals. These electrons may be paired (no magnetic field), or unpaired (a magnetic field exists). When a material is placed in a magnetic field, its extent of magnetization can be described by magnetic susceptibility. Three categories exist to define the magnetic susceptibility, they are: diamagnetic, paramagnetic, and ferromagnetic. Most organic materials and water are examples of diamagnetic materials. They have slightly negative susceptibility and oppose the magnetic fields (Bushberg 2002). Paramagnetic materials will enhance a local magnetic field, but they in and of themselves have no detectable self-

magnetism, medium susceptibility. Examples of paramagnetic materials would include molecular state oxygen (O₂), and gadolinium-based contrast agents. Materials which are said to be ferromagnetic increase substantially the magnetic field; they have a high susceptibility. Ferromagnetic materials include cobalt, iron, and nickel.

A hydrogen nucleus is often referred to and will be referred to hereafter as a proton. Protons have an associated *spin*. As a spinning charged particle, it also produces a magnetic force. Each proton creates a tiny magnetic field called a magnetic moment. Detection comes from measuring the protons in large numbers. Thermal energy in tissue randomizes the direction of the spin. Once placed in a strong external magnetic field the protons align with the applied field in one of two states, parallel or antiparallel (the higher energy field). The energy separation of these two magnetic states increases with magnetic field strength (Bushberg 2002). Those protons that have magnetic moments in line with the magnetic field have an energy state that is lower than those aligned opposite the magnetic field. The excess nuclei in the lower energy state determine the overall net magnetization of a patient.

In classical physics we say that the applied magnetic field causes the protons to experience a torque similar to when a spinning top wobbles because of the gravitational force. The rotating characteristic that can be described as a wobble is called the precession. This term comes about because they are actually oriented at an angle to the magnetic field and thus precess around it. Visually represented, this precession would appear as a cone around the bulk net magnetization. The frequency of precession, ω_0 , can be calculated using the Larmor equation (Bushberg 2002):

$$\omega_0 = \gamma * B_0 \quad (\text{Eq. 2.1})$$

where B_0 is the strength of the external magnetic field in tesla (T) and γ is a constant and unique for each type of nucleus, known as the gyromagnetic ratio.

The above description is the classical description of magnetic moments, and when analyzed deeper, isn't completely accurate. Quantum mechanics gives a more accurate description of what occurs with magnetic moments and their interaction with a magnetic field. Every nucleus has a quantity called *spin*. The spin value is quantized in half-integer units called spin quantum numbers. This number dictates many of the MR properties of a given nuclear group, and limits the number of ways a nucleus can spin. The *nuclear magnetic moment* is the magnetic field associated with the spinning charged particle (Bushong 2003). Hendee and Ritenour tell us "In the region of the atom, where distances are small and the 'discreteness' of energy levels and angular momentum is apparent, it is not possible to predict the exact behavior of individual atoms with certainty" (2002). Because angular momentum and energy are available in discrete values, or precise allowed states of spin, the image of a top spinning smoothly on the table surface isn't exactly true. Quantum mechanics also refers to photons or packets of electromagnetic energy instead of using the term "waves". Just as Bushberg gave us the Larmor equation (Eq. 2.1) to calculate the frequency of the interacting radio wave, the quantum model provides an equation to calculate the energy of the photon using the determined Larmor frequency. This equation is given as:

$$E = hf \quad (\text{Eq. 2.2})$$

where E is the energy of the photon, h is Planck's constant, 4.14×10^{-15} eV-sec; and f is the Larmor frequency measured in Hertz, or cycles per second (Hendee and Ritenour

2002). This energy calculation tells us how much energy is required to cause transition between low and high energy states.

The precessional frequency, also known as the Larmor frequency, for a proton is 42.58 MHz in a 1-T magnetic field (Bushberg 2002). For the 3-T magnetic field used in this study, the precessional frequency for the proton is 127.7 MHz.

To begin acquisition of images, radiofrequency (RF) pulses are sent into a patient located within the magnet. These are short bursts of electromagnetic waves sent in to disturb the alignment of the protons. Only RF pulses equal to the Larmor frequency will exchange energy and cause a change in proton alignment. This causes the net magnetization to flip toward the transverse plane, resulting in a decrease in longitudinal magnetization (Schild 1992). The hydrogen nuclei are then aligned against the magnetic field in the anti-parallel position, and precess “in-phase”. Once the pulse is switched off, the whole system begins to revert back to its original position. The recently formed net transverse magnetization disappears, and longitudinal magnetization returns (Schild 1992). The net magnetization vector, M , rotates by a specific distance or angle. The degree to which the RF pulse displaces the net magnetization vector from the Z axis is known as the flip angle. The RF pulses used in MR imaging are named for their flip angles. An 180° RF pulse causes a flip angle of 180° , and the same relationship holds true for a 90° RF pulse. The movement of the vector, M , in the transverse plane produces a voltage in the receiver coil. As M returns to equilibrium, the signal weakens, or decays. This decay is known as the Free Induction Decay (FID), and is the signal itself produced from the excited hydrogen atoms (ICPME 2001). This can also be described in terms of quantum mechanics. When a system of nuclear spins is at

equilibrium with the external magnetic field, electromagnetic radiation, when introduced, will disturb the population and nuclei of a lower energy state absorb the energy. This causes them to excite into the higher energy state. As this energized group of nuclei slowly return to their original groups, an observed signal is emitted; known as the MR signal (Bushong 2003).

The time required for the longitudinal magnetization to recover is described by the longitudinal relaxation time, T_1 , also known as spin-lattice-relaxation. This is not an accurate measure of time per proton, but a description of time for the whole process to occur. Another time constant, known as the transversal relaxation time, T_2 , or spin-spin-relaxation and is due to the proton precession at slightly different frequencies. This relaxation coupled with the inhomogeneities of the magnet cause the FID to decay more quickly (T_2^*). The differences in T_1 , T_2 , and T_2^* are what provide the high contrast in MRI and are important when considering what needs to be seen in the acquired images (Bushberg 2002). T_1 is very dependent on the make-up of the tissue and its structure. Water, for example, has a long T_1 value, because the smaller water molecules move very rapidly and energy exchange is difficult. The more median sized molecules contained in the lattice, the shorter the T_1 . An example of a short T_1 would be fat tissue. Energy is transferred to the lattice very efficiently because of the precession of the carbon bonds at the ends of fatty acids. T_2 relaxation occurs because protons dephase due to the local magnetic field differences. Larger differences in local magnetic fields cause larger differences in local precessional frequencies. Protons dephase faster due to these larger differences, which in turn leads to a shorter T_2 .

A series of RF pulses is called a pulse sequence. The choice of the pulse sequence will determine what tissues will have large or small signal intensity. There are three types of images that are most common in MR imaging; they are T_1 -weighted, T_2 -weighted, and spin density weighted. When choosing which one produces the desired image content, one must determine if tissue contrasts are best seen by T_1 , T_2 , or spin density. By using different combinations of TR and TE, one can emphasize differences in the tissue contrast of the acquired images.

There is a direct correlation with blood flow and the body's activities, or response to external stimuli. It was discovered in 1990 by Ogawa and colleagues at the AT&T Bell Laboratories that mapping brain function was possible by using the venous blood oxygenation level-dependent (BOLD) MRI contrast (Faro 2006). Just as changes in tissue composition lead to T_1 , T_2 , or spin density weighted images, the changes in concentration of deoxyhemoglobin (dHb) levels in the blood, change the signal intensity received in MR imaging. The dHb acts as a paramagnetic contrast agent, and since it is already found within the body, it is considered endogenous. The idea of using what the body already provides creates a way of imaging functionality of localized brain areas without the need to inject an exogenous contrasting agent. The use of the BOLD signal technique to image neuronal response has come to be the basis for what is known as fMRI (Price et al. 2002).

It is important to note that only venous blood can contribute to activation induced changes when dealing with the BOLD contrast (Faro 2006). The venous blood is the blood that contains deoxyhemoglobin; it is the blood returning to the heart after circulating through the arterial system, and constitutes 75% of the total blood volume in

the body (Faro 2006). While a strong signal originates from the venous blood supply (an intravascular component), it is also known that the gradient-echo BOLD contrast or signals also arise from extravascular components.

The largest source of extravascular signal contribution is from the water in tissue surrounding the blood vessels, with a greater local response from the larger vessels. Smaller vessels also give a response, but because they are small the signal received involves a dynamic average over many different fields (Frahm 1994). The larger vessels have a dynamic average over a local position. This is due to the fact that during echo time in fMRI, water molecules are known to diffuse $\sim 17 \mu\text{m}$, creating a dominant dephasing effect. Many fMRI images of neuronal brain activity will have non-site specific areas of activation, mostly due to the larger draining veins. At higher magnetic fields, the venous related signals can be minimized; this compromises spatial specificity. Gradient-echo pulse sequences are used in fMRI to increase the sensitivity of the system.

Two forms of resolution need to be discussed when dealing with fMRI. These two areas of interest are temporal and spatial resolution (Kim 1997; Menon 1999; Faro 2006). One issue of concern is that of the draining veins. Small capillaries drain into larger vessels which may create an additive effect of the BOLD signal. This may be compounded on top of the signal due to the amount of blood in the draining vein being significantly larger than that of its relative capillaries. These effects are contributors to spatial misregistration. It is this spatial misregistration that can cause a signal to appear outside of the suspected area of activity, or even outside of the acquired image (Faro 2006). The use of higher field strengths will also reduce contributions from the venous system when compared to the areas of true cortical activity.

Spatial resolution is not only dependent on signal-to-noise ratio (SNR), but also to hemodynamic response (Faro 2006). Even though images may be obtained quickly, the body's hemodynamic response is relatively slow. Hemodynamic responses can appear anywhere from one to two seconds post stimulation. These response times vary proportionally with a person's age. Temporal resolution is limited by these factors mostly because the majority of acquisitions are performed using a block design. The block designs, or patterns, repeat themselves in cycles, often with long stimulation phases.

Identifying prominent areas of olfactory reception by creating a practical and simple imaging protocol is what my research emphasizes. All imaging was completed using a Philips 3-T MR Spectrometer.

Our goal is to develop a consistent quantitative study to determine if fMRI can be used effectively for the diagnosis of olfactory dysfunction. Those results may lead to better quantification of the areas of the brain that have the strongest activation regions in a given population.

CHAPTER 2

MATERIALS AND METHODS

This study was performed with IRB approval and was HIPAA compliant.

Research of olfactory neurological response is difficult due to the various anatomical parts of the brain that are involved in the smell process in addition to responses not due to olfactory stimulation which may occur during the scan. The position and comfort level of the patient being imaged are factors that had to be taken into account while imaging neurological responses, as the brain is recognizing a diversity of external stimuli within the same time frame. A Philips 3-Tesla MR spectrometer was used to acquire all images in this study (Fig 2.1). Like all closed MRI scanners, it consists of a long narrow bore in which the patient was placed. Each patient was oriented head first in the supine position. The individual was given a set of sponge-like ear plugs that were placed inside the external auditory canal, with a pair of headphones placed over the ears to further minimize distraction from the loud noises incurred from routine function of the MR scanner. Extensive functional MRI research has been done on 0.75-Tesla and 1.5-Tesla scanners, with very little work done on 3-Tesla systems.

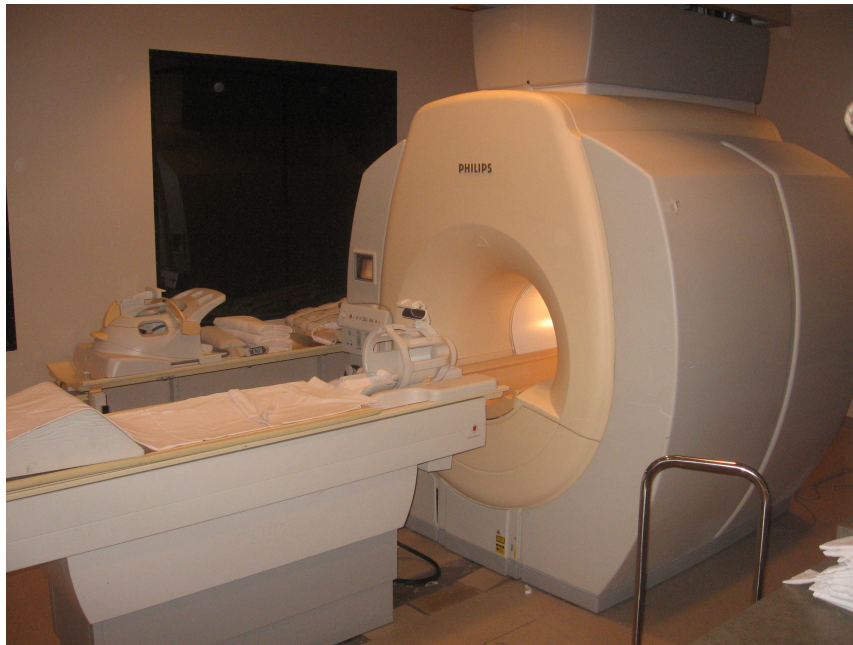


Figure 2.1 The Philips 3-Tesla MR scanner at NIC-Rainbow, Las Vegas, Nevada.

The patient was positioned as comfortable as possible; which included the placement of a triangle wedge under the knees for proper alignment and comfort of the spinal column, and a blanket to keep warm if requested. Once positioned, an 8-channel head coil was placed over the head. To minimize unwanted external stimuli, each patient was asked to lay still, eyes shut, with their hands positioned, either to their sides, or resting together on the abdomen. By keeping the hands down and relaxed, the brain's sensory-motor responses were minimized. Visual stimulation was minimized by shutting the eyes throughout the length of the scan and by turning off the internal light of the MR scanner. Auditory stimulation was decreased with the aid of three factors; first the use of internally placed ear plugs, second the use of external headphones, and third the use of white noise, or static, transmitted through the earphones. The goal was to keep all non-olfactory stimuli to a minimum as much as physically possible.

Delivery Device Development

The first task was to create an apparatus that could deliver desired scents to the subject's nasal passageways. The device could not be too cumbersome while, at the same time, meeting the demands of the physical characteristics of a 3-Tesla magnet. It is a common practice in healthcare to use nasal canulas, or oxygen masks, for the delivery of oxygen to patients who are not breathing adequately on their own. Oxygen masks vary in size and shape, as well as in functional characteristics. Some masks allow air to circulate freely in front of the nasal and oral cavities, while some force a controlled amount of air into the nasal passages. Nasal canulas provide the most space efficient way of delivery, but we realized a discrepancy in how to deliver multiple scents through a single line without cross-contamination. We began our delivery of oxygenated air with the use of an oxygen mask connected to a PVC adapter that permitted the placement of three independent oxygen tubes, see Fig. 2.2. Two of the oxygen lines were used to usher in desired scents, while the remaining line allowed for the delivery of fresh, unscented oxygen.



Figure 2.2 Delivery Mask with three separate oxygen lines entering through a PVC adapter.

The two oxygen tubes that were isolated for the flow of scents were connected, at the other end, to a small box made of PVC, (Fig. 2.3), which housed the chosen scents.

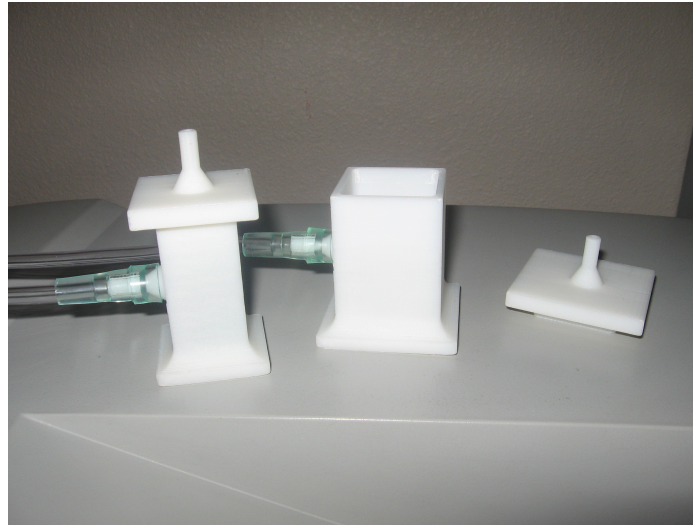


Figure 2.3 Scent-containing Boxes. The oxygen enters through the side inlets, mixes with the scents contained inside, and then exits to the patient through the outlet in the top.

Inside the boxes were placed multiple 2x2 gauzes that had been saturated with a liquid form of a desired fragrance. Each box had an entry port placed in the lid for incoming unscented oxygen as well as an exit port for the outgoing scented oxygen. The individual scents themselves were administered in an alternating pattern. This was done with the idea that too much of one scent may saturate or overwhelm the olfactory receptors. Between alternating scent patterns, a period of pure oxygen was introduced to try to clear out residual or lingering scent in hopes that the receptors could be stimulated repeatedly.

The flow of oxygen in the tubing from the oxygen tank to the scent boxes was controlled by a valve that was connected to a filter. This charcoal filter was placed in the entry tubing of the oxygen line to filter out any scent originating from the oxygen itself.

This filter was placed just beneath the regulatory valve, Fig. 2.4. The valve made it possible to direct the air flow into the scent-containing PVC boxes, in repetitive cycles; thus controlling the input of oxygen each box received, which directly affected the amount and time of scent administration. The main flow of oxygen was regulated at a flow rate of 2.0 liters per minute (Lpm). The overall delivery cycle followed this path: oxygen was released from an MRI compatible oxygen tank, flowing next through the charcoal filter to the control valve. The control valve was manually operated to release oxygen at specified times to the scent-containing boxes. The scent boxes had the carbon-filtered oxygen blown into them through standard oxygen tubing. The air circulated within the box, mixing with its respective stimulus odors, before leaving through an exit tube in the lid. The oxygen left the box, carrying with it small particles of the contained scented liquid, and traveled to the delivery device affixed to the frame of the 8-channel head coil. The oxygen and stimuli were forced to the contained area inside the mask, where it was taken in and processed by the receptor sites in the brain. The overall set-up can be visualized in computer-generated form, Fig. 2.5, below.



Figure 2.4 Control valve with charcoal filter that filters the incoming air from the oxygen tank. The two oxygen tubes leaving the through the side of the valve, channel the air flow to the scent boxes.

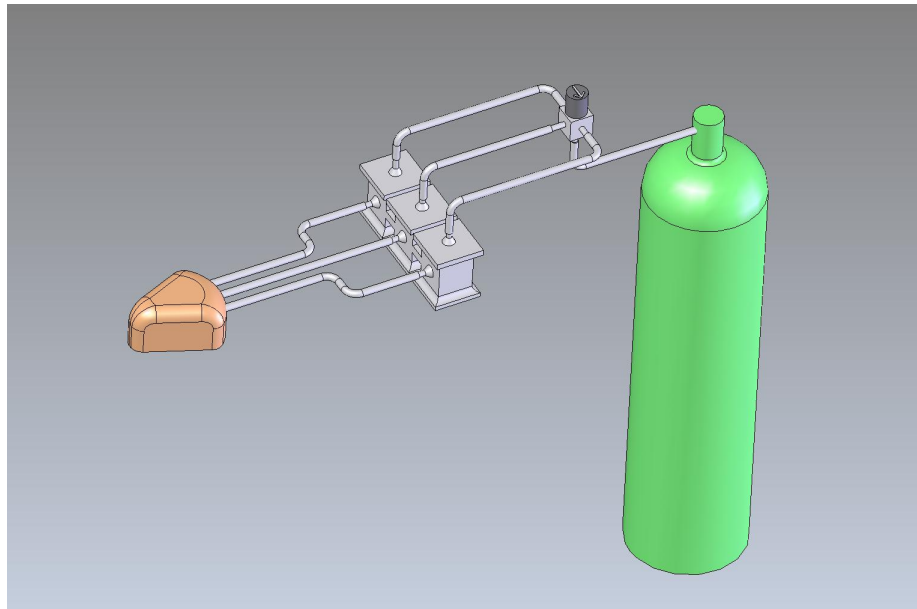


Figure 2.5 Delivery Set-up showing the path oxygen takes from the tank, through the air valve, into the scent boxes, and finally to the patient via an air mask or delivery device.

Other devices were developed that could accept multiple delivery lines and yet be modest and accommodating in size and shape. These devices were made out of PVC and tested in different styles. The idea behind them was the same as the breathing mask; to allow multiple lines of scent delivery to the nasal passages. In creating these devices, the advantages and disadvantages of each piece were considered. Fig. 2.6 shows an example of a delivery device that could be positioned in front of the patient by firmly biting down on an extension at its base. Four intake holes are located on the sides of the device for the placement of oxygen tubing. The airflow would be directed in through the sides and then forced out through the top. The exit holes included a slanted floor which directed the flow of air toward the subject's nose.

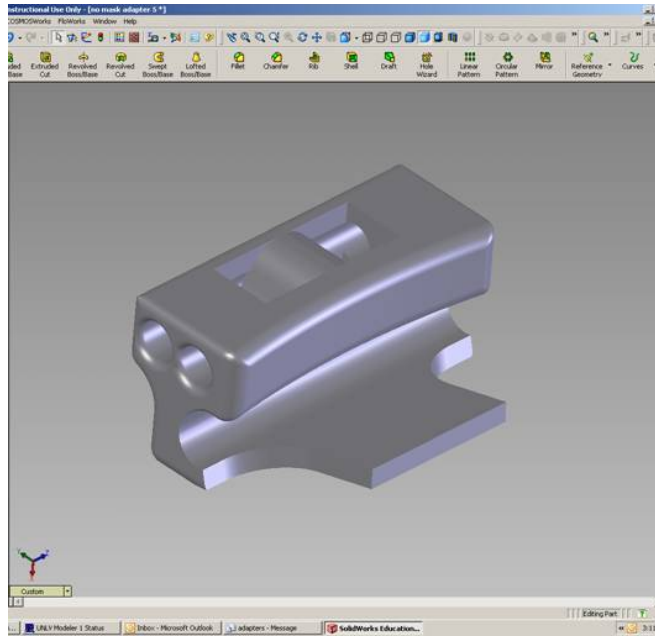


Figure 2.6 Delivery device with superior air release and a bit plate to position the device directly in front of the nasal passages. The oxygen tubes enter the device through the two round holes located on each side.

Another PVC delivery device created was formed with the idea that it could be connected to a head band, or piece of elastic, and secured to the patient, by being wrapped around the head similar to the oxygen mask. Oxygen tubes would enter in through the side openings and exit through the top exit holes, forcing the air out into the nasal passages. It would rest between the patient's upper lip and the base of the nose. This device is seen in Fig. 2.7 without the elastic string attached. The flooring of the exit holes is sloped out to help direct the flow of air into the nostrils.

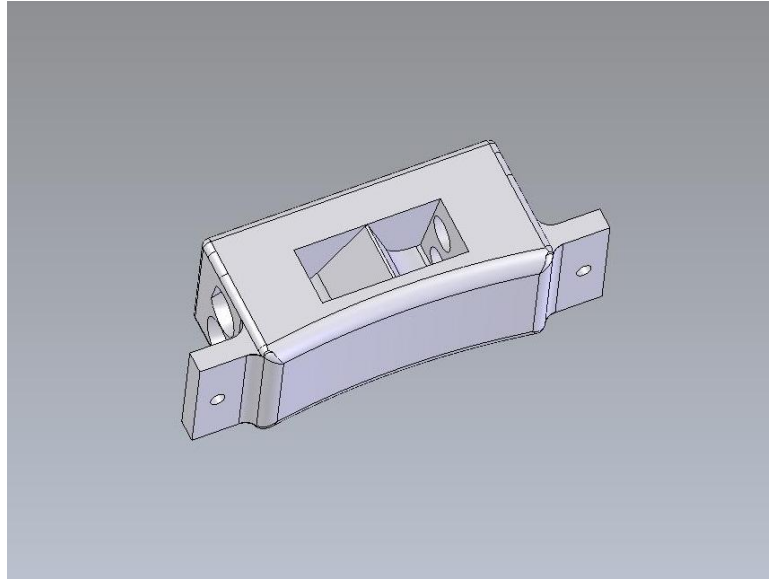


Figure 2.7 Secured scent delivery device with places to secure an elastic string at each side. The elastic would then wrap around the patient's head, keeping it securely in place between the upper lip and the base of the nose. The oxygen tubes enter through the sides and air is released through the top exit holes.

A third compact delivery device was developed with the idea that the device could be secured to the head coil and not come in direct contact with the subject being imaged. It was designed with the same purpose, but included flow-directed exit canals aimed toward the nasal passages. Figure. 2.8 shows this device placed on the midline cross-bar of the MRI head coil. The oxygen tubes enter through the front of the device, which allows them to be directed to the rear of the scanner where the oxygen source and scent boxes are located. The device was secured to the head coil by using a small sample of plumber's putty to keep it from sliding or repositioning itself with the motion of the bed in and out of the scanner. Placing the scents in the direct path of respiration was designed to increase the chances of recognizing and quantifying receptor site stimulation. Figure. 2.9 shows the conceptual rendering and design of this device.



Figure 2.8 Coil mounted delivery device. Oxygen tubes come through the bore of the magnet, entering the device through the caudal end. Oxygen is passed through the tubes and released through the inferior holes, forcing the air in the direction of the nostrils.

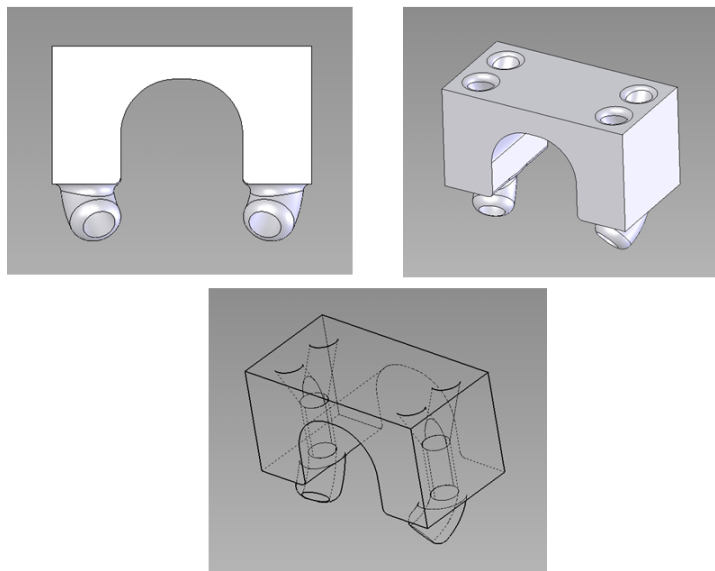


Figure 2.9 Design concepts for the Coil-mounted Delivery Device seen in Fig. 2.8, but with oxygen tube inlets positioned on the top of the device. This made the device more cumbersome and ultimately the caudal end access holes were used.

With the patient in the head-first supine position, the delivery device was fastened to the head coil with oxygen tubing extending toward the back opening of the MR scanner. The oxygen tubing was connected to the lids of the scent boxes. To minimize the distance required for air to travel in these lines, the scent boxes were placed near the back edge of the MRI bore. The scanner itself created a vibration factor that required a sandbag be placed behind the boxes to help maintain their position near the back of the bore. Oxygen tubing was attached to the posterior aspect of the boxes and extended to a manual valve, the one identified in Fig. 2.4. The person responsible for turning this valve, the valve mediator, had to cooperate fully with the person running the acquisition computer, the controller. The controller signaled to the valve mediator when to engage oxygen flow, when to switch from one scent to another, and when to cease oxygen flow. The biggest advantage to doing this manually was that the valve mediator had total control and could accurately verify that air flow was progressing or not. An automated system would be ideal, but technical problems are likely to arise. The negative side to having a person rotate the valve is that more manpower is required.

Image Acquisition

All images were initially acquired using Philips Intera software with IViewBold, release 1.5, and later Intera software version 2.5. Every image set that was acquired for information included multiple types of scans. The initial scan was a survey showing placement of the head within the coil, or field of view. The second scan was that of a “SENSE Head”. The SENSE (Sensitivity-Encoded) scan couples the head coil to the magnet itself and increases the quality of the scan. A T1 weighted 3D sagittal view was

obtained to show the brain anatomy. After the anatomical acquisition, fMRI acquisition started. The fMRI protocol details changed over time, but consistently showed the hemodynamic response of the brain from the given RF pulses and smell stimuli. Table 2.1 identifies the scans of the actual acquisition protocol and what the purpose was for each scan.

Table 2.1 olfactory fMRI scan protocol with simple description for each portion of the scan. Each part of the overall scan is labeled as “Scan Title”.

<i>Scan Title</i>	<i>Scan Description</i>
SmartBrain	This is the surview that allows for positioning of the markers for brain acquisition
SENSE head	This is the scan that couples the 8-channel coil to the magnet
T1Wref_FMRI	Reference scan for single shot fMRI that can be used for anatomical underlay on acquisition workstation
FMRI/Olfactory	T2* weighted image that demonstrates BOLD activated regions
T1W/3D/Sag	Anatomical image for underlay of the activated regions

Protocols for other functional studies, which had already been established by the Philips software team, were sampled. Some of these protocols involved auditory response as well as sensory motor response. This testing of the protocols created the baseline idea of where to initiate our own olfactory protocol design. For many of the first acquired images, a block pattern of imaging dynamics similar to those used in the auditory fMRI sequences was arranged. The administration of scents was done in cycles which included a thirty second “on” period followed by a thirty second “off” period. During the “on” phase, the control valve was used to alternate between administering two

different scents in three to five-second intervals. The “off” cycle had no scent administered and the subject was left to breathe room air. These cycles were each repeated multiple times during the fMRI scan for a total acquisition time of five minutes. Some of the things considered were the individual scents, the delivery location to the subject, ambient stimuli, and the odors given off by any of our supplies, including the new oxygen tubing. With the initial software, one was able to generate desired scent delivery protocols with ease. A dynamic block system was used to tell the scent regulator when a scent was to be given, when a scent had been turned off, and what to subtract out as background to improve or increase the signal to noise ratios. This is demonstrated in Fig. 2.10, with each rectangle representing a dynamic or interval of acquisition. The gray shaded blocks identify when that command was enforced with respect to the overall image set. During these initial scans, 64 dynamics, on average, per image set were acquired. The number of dynamics acquired varied throughout the study from twenty to eighty.

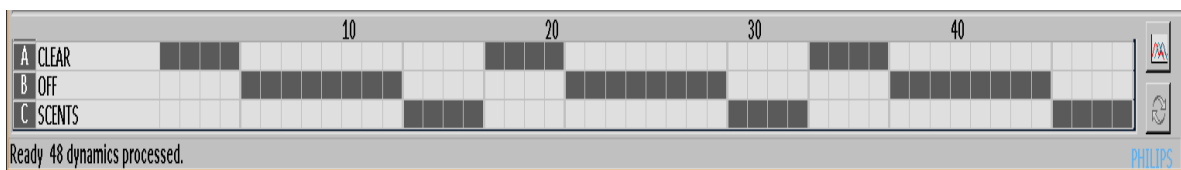


Figure 2.10 An example of a three-command form of Dynamic Block Acquisition. Each block, or dynamic, represents a time interval with a predetermined TR value. A scent was introduced during the “SCENTS” segment of the functional acquisition.

After 5 months of data collection, Philips installed a newer version of the Intera software, 2.5, that altered the acquisition parameters, making them more difficult to manually regulate. A considerable amount of time was spent trying to determine the

method used by the computer to compare activation to no activation. With the previous version the paradigm could be created by identifying each stage of acquisition. The “on” stage was when a scent was administered. The “off” stage represented the time where no scent was being given. A third stage titled “clear” was instituted to compensate for time required for the olfactory responses to stop after the scents were turned off. Time was required for the registration of the scent to deregister before a new scent was given. The “off” stage, and its associated values, was considered the background necessary to compare with the activated values. To obtain an image for activation versus no activation, the “on” dHb concentrations were simply subtracted from the “off” dHb concentrations and the “clear” dynamics were ignored completely to get a better clinical understanding of the receptor site activation.

However, the upgraded software did not allow for the exclusion of any dynamics. Along with this new software came the ability to view the functional response during the actual acquisition. This made it possible to generate an image of the subject’s functional response as it was acquiring. It was then able to be reconstructed or analyzed further using other fMRI post acquisition processing software.

The images used to display the activation regions are T2* weighted with TR values determined based on the subjects breathing patterns. TR values were determined through manual observation of the subjects breathing cycle while in and out of the scanner. Some images were acquired with a TR set as high as 5000ms and as low as 2000ms. The breathing cycle among all subjects was determined to be an average of 3500ms, allowing us to select this time as the TR for our scan and include the shortest TE possible, around 35ms.

Initial images included slices of the majority of the brain with slice thicknesses that varied from 2mm to 4mm. Ultimately the focused region of interest was isolated to the portion of the brain known to contain the olfactory bulbs, olfactory tracts, and the limbic system, with a chosen field of view, FOV, of 230mm. The number of slices used was thirty at an angle parallel to the cantho-meatal line.

A variety of scents was chosen that could, ideally, identify those that would give better overall responses. In the beginning the following scents were rotated through: vanilla, cherry, pine, mango, brown ale, and isopropyl alcohol. Using the chosen scents, it was identified which were most obvious and easiest to recognize. It is important to note that different smells will have an effect on more than just the olfactory receptor sites themselves.

Not only is the scent itself an important consideration in identifying receptor sites, but the breathing patterns of the subject as well. All subjects were asked to maintain a normal, consistent breathing pattern throughout the duration of the image acquisition.

Image Processing

Imaging software played a vital and challenging role in the ability to acquire useable data. Once data was acquired, the processing software allowed for analyzing and quantifying the response centers of activation. All images that had been acquired were sent to a processing work station where the data was processed with the fMRI software, Brain Voyager QX¹. During the processing, the individual intervals of the acquisition were isolated, or identified, by creating stimulation protocol files. Stimulation files, or

¹ Philips' BrainVoyager QX Version 1.10.4.1248
Copyright © 2001-2009 Rainer Goebel

predictors, allowed the user to identify the “on” and “off” periods during acquisition and display them on a signal-time course plot. These files were used to help in the statistical analyses of data. The power of statistical tests was further strengthened by “preprocessing” the data (Goebel et. al. 2008). The preprocessing removed drifts in signal time courses and aided in removing artifacts caused by head motion. Linear correlation maps were created and specified general linear models were fitted to the processed time courses to help explain whether or not the model actually fit the time course. Color schemes were assigned in the processed images to better help show where the predictors should have been detected.

The activated regions were then analyzed with regions of interest, ROI's. The ROI software used statistical data to show how well the general linear model fit the data. P-values were also used to determine a probability value for the significance of the data. The analysis made it possible to identify which areas of the brain were most likely activated due to the administration of the olfactory stimuli in all patients. An outline of the steps followed for the processing of each brain on the BrainVoyager software is found in appendix B.

CHAPTER 3

RESULTS

The loss of smell has come to mean more than just a failing organ system. It has been shown to have implications with various forms of dementia, including Parkinson's disease and Alzheimer's. Months of studying the olfactory process with fMRI has yielded the following results.

Delivery Device and Set-up

In order to test someone's ability to recognize an odor, a scent was delivered to a person in such a way that it could pass into the nasal passages and up to the olfactory bulb. The first device utilized for scent delivery was the full oxygen mask as seen in Fig. 2.2. While the mask was the best way of isolating the scent to the facial area for breathing purposes, it did not provide a sufficient release of air; causing satiation of cells for a longer period of time, or a lingering of the scent in the breathing region as demonstrated by the signal response shown in Fig.3.1. For every scent that is detected, there is an initial saturation response before another scent is detected. This saturation response usually lasts 2.5 to 3.5 times the length of scent duration, thus making it crucial to separate activated time frames with sufficient time to allow for the brain to recognize further changes in blood oxygen levels.

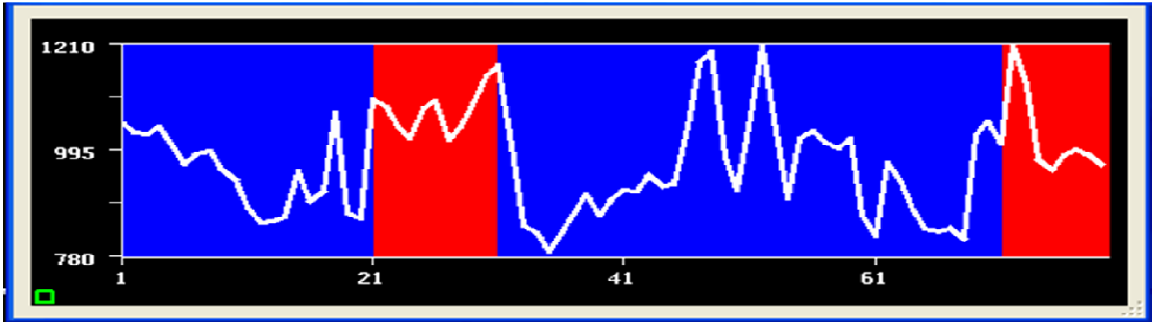


Figure 3.1 An example of a signal-response graph with red representing scent-activated time intervals, and blue representing non-activated time frames. These two spikes in the blue region are due to the scent being trapped in the mask.

The bite plate model, as seen in Fig. 2.6, delivered the scent directly to the nasal passages, but some problems included the fact that the individual pieces either required disposable bite plate covers, which could be costly, or that the patient may alter the bite pressure during the scan causing increased activation in some areas of the brain. Another device utilized was the secured device as seen in Fig. 2.7. The elastic string attached to the device which wrapped around the patient's head secured it in position directly beneath the nasal passages on the upper lip. The positioning made it difficult for coil placement on some patients with larger heads, as well as an irritation for the subject while breathing. Other delivery devices, such as the one that blew the air down and not toward the nostrils, did not get the scents close enough to the nasal passages to be considered a sufficient amount for recognition, see Fig. 3.2.

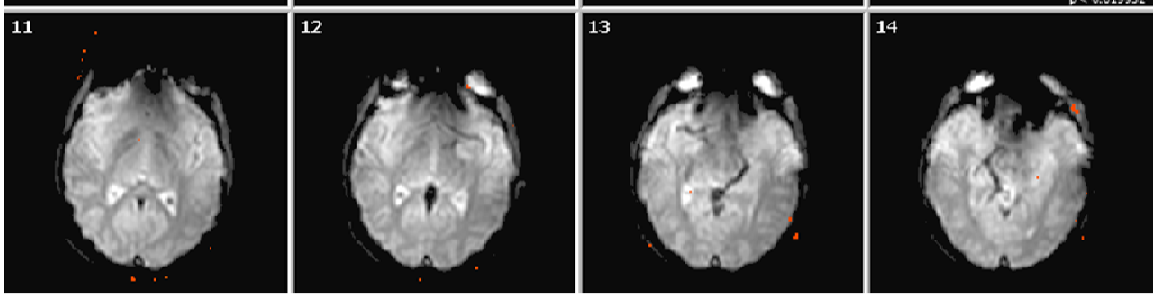


Figure 3.2 This image shows very little activation sites, some eye movement and some statistical noise near the scalp. There is no activation in any of the olfactory bulbs or limbic region.

After many prototypes, the delivery device mentioned in Chapter 2, Figs. 2.8 and 2.9, the open-ended flow circuit aimed in the direction of the nostrils, was chosen as the best device for use in this research project.

Once the device was created and positioned for delivery, an acceptable oxygen flow rate was determined. An air flow rate of 4.0Lpm caused some to physically jerk, creating motion artifacts of the head and neck as well as functional response from the eyes and facial motion. The elevated level of flow also made the subjects uncomfortable; affecting their breathing patterns and eye movement. Even though all persons remained with their eyes closed, repeated ocular activation was identified in these images. An example of an unexpected functional hemodynamic response can be seen in Fig. 3.3 with its signal response graph.

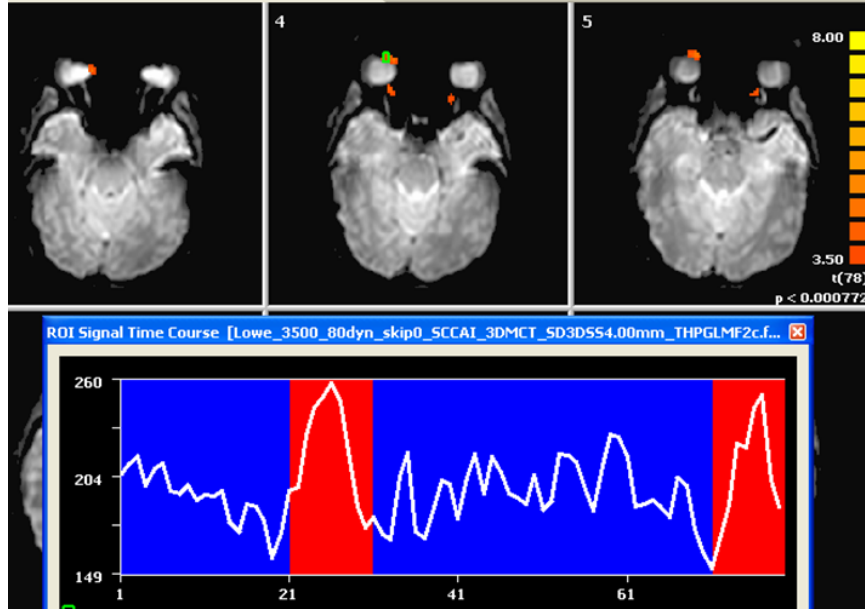


Figure 3.3 The Signal-Time Course graph represents the response of the anterior aspect of the right eye in the above image. Increased signal within the red dynamics was probably due to motion at initiation of the scent.

When the flow rate was too low, between 0.5 and 1.5Lpm, subjects had a difficult time identifying that there was even a scent being administered; as the air in the vicinity was inseparable from the ambient room air while the air conditioner or fans were in use. Some of those who anticipated the scent's arrival actually tried to sniff harder to identify the new smell. The ideal flow rate was determined to be 2.0-2.5Lpm. At this rate, all subjects were comfortable with the introduction of air flow so as to not distract them from their breathing patterns, yet sufficient enough to deliver a recognizable scent.

Consistent breathing patterns were difficult to maintain for some. Without a respiratory gate in place, the breathing patterns of our subjects were timed and an average breathing cycle was determined to be seven seconds, making the inhale and exhale portions 3.5 seconds each. This time was used to establish the TR value for acquisition parameters.

Data Acquisition and Processing

Imaging paradigms in a block pattern were used to acquire functional data. Image data, acquired using Philips' IViewBold software², gave a real-time look as to the activation responses. These could then be analyzed by drawing regions of interest (ROI's) around desired activation spots. Results varied greatly, and artifacts were identified periodically. Much of the diagnostic results come from ROI evaluation as well as through the processing of *.par and *.rec files using the BrainVoyager QX software³.

One of the earliest paradigms used as a starting point for creating an olfactory protocol was a five minute sequence broken up into thirty second intervals. For the first thirty seconds, the subject was left breathing pure oxygen. At the 0:30 mark, the controller gave the command to initiate the release of the scent to the subject. The valve was switched on and rotated back-and-forth between scents; initially cherry, lime, lemon, strawberry, or pine, every five seconds for thirty seconds, to diversify the scent and try to minimize satiation of the olfactory receptors. At the end of the thirty seconds, the delivery valve was turned to the off position and the subject was returned to pure oxygen. This process continued until the five minute acquisition was complete. With the time frames of stimulation equal to those without, a period of sensory de-stimulation did not occur. With each activation, the background levels rose higher and higher creating an unacceptable visual result of response.

The second set of paradigms tested, consisted of lengthier activation periods. They consisted of ten second scented intervals over a thirty second period; maintaining the five minute total scan length, with clean oxygen for a period of thirty seconds

² Philips IViewBold Software version release 1.5

³ Philips BrainVoyager QX Version 1.10.4.1248

Copyright © 2001-2009 Rainer Goebel

between scents. With such an extended exposure to smells, it was shown that the activation response was strongest in the beginning seconds of acquisition as in Fig. 3.4. However, the number of data points that were sampled at this time was too low to successfully isolate the olfactory region, suggesting a continual activation even during the “off” phases, or a loss of activation during the “on” phases.

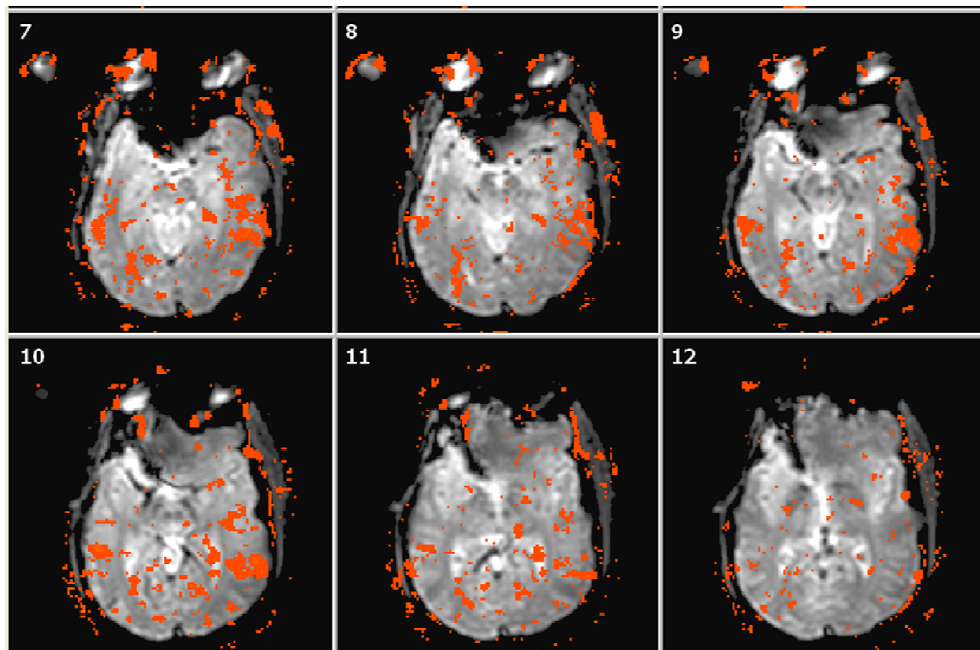


Figure 3.4 An example of increased activation in the early stage of scanning with a prolonged “on” set of dynamics.

The activation tapered off dramatically over a short period of time as seen in Fig.3.5, again suggesting a decreased activation in the “on” phase due to inter-interval saturation or intra-interval saturation.

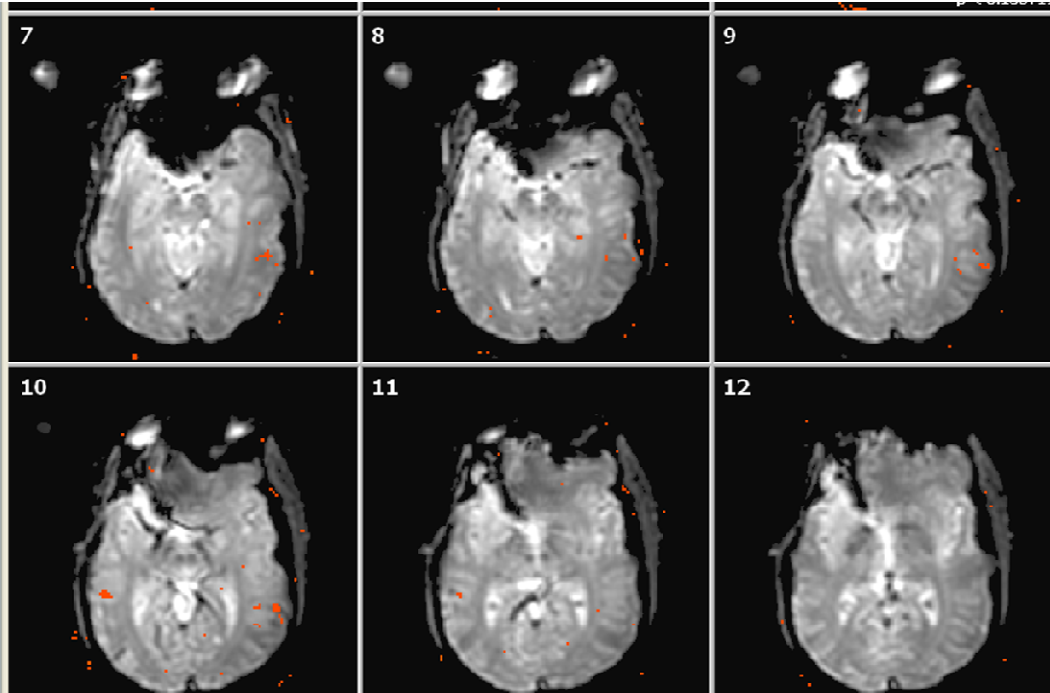


Figure 3.5 an example of decreased activation in the later stage of scanning with a prolonged “on” set of dynamics. Notice the extreme decrease in areas of activation when compared to the images in Fig. 3.4.

To aid in the processing of the data, certain dynamics were excluded to account for receptor site saturation. This phase of acquisition was titled the “CLEAR” phase as explained in chapter two. This gave more statistical importance to the dynamics where the scent was actually delivered; which in turn gave a better quality image.

The new upgrade made it possible to watch a “real-time” response to the functional scans. Reconstructing on the acquisition computer was convenient, but didn’t allow for sufficient analyzing of the data. An attempt was made to set up the functional acquisition similar to before the upgrade by establishing three separate commands, on, off, and clear. The inclusion of a third command, clear, seemed to complicate the reconstruction process by confusing the application on which dynamics would be used as the baseline. This clear phase, seen in Fig. 3.6, was thought to be ignored, and therefore

improve the signal to noise ratio. But the evaluation of its function was inconsistent, and later determined that only two phases could be applied to any one protocol. It was determined impossible to manually ignore those dynamics representing the saturation effect and BrainVoyager⁴ had to be utilized for all processing.

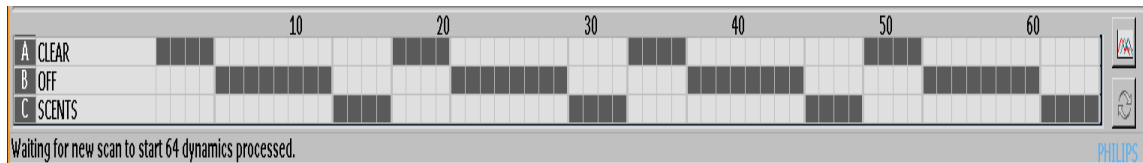


Figure 3.6 Three individual segments on a 64 dynamic acquisition showing the clear phase as four dynamics, repeated four times over the course of the scan.

With the new upgraded software, some lapses in response were identified based on the subjects breathing cycle. An attempt was made at applying a respiratory gate. This respiratory gate allowed the subjects breathing cycle to be monitored and used in the acquisition of the images. It aided in regulating the delivery of the scents. One major inconvenience was that the scan time increased three fold. This was based on the need to wait for a regular breathing pattern; the more regular, the more fluid the scan. The increased time did not make the scan clinically practical, regardless of the results.

Response to Different Scents

Different scents were tested to try and identify the best response. These other scents included mango, banana, dill, tabasco sauce, cinnamon, brown ale, and isopropyl alcohol. The ale and the alcohol gave the best responses of these seven scents. While the

⁴ Philips BrainVoyager QX Version 1.10.4.1248
Copyright © 2001-2009 Rainer Goebel

limbic system is a known area of the olfactory system, there was an interesting occurrence of an increase in activation of the thalamus gland, most noticeable with the administration of the alcohol products. Figure 3.7 shows an example of activation after having smelled brown ale and isopropyl alcohol. It is not known why there was increased activation with alcohol versus other scents, but in this study, no other scent created as much activation as isopropyl alcohol in this location.

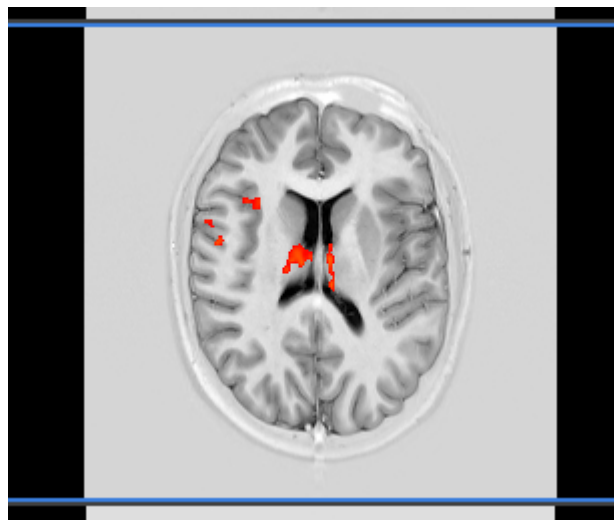


Figure 3.7 Brain activation of the thalamus after the scent of isopropyl alcohol was administered

Another interesting extreme was an over response when Tabasco sauce was administered under an increased flow rate as shown in Fig. 3.8. Typically the olfactory response is seen within the limbic system, nasal passages, and frontal cortex. Activity in the following images can also be seen in abundance in the right hemisphere near the superior sagittal sinus, the parietal lobes bilaterally with right greater than left, the

insular cortex bilaterally, the visual cortex, and in the region of the midfrontal gyrus higher up in the brain.

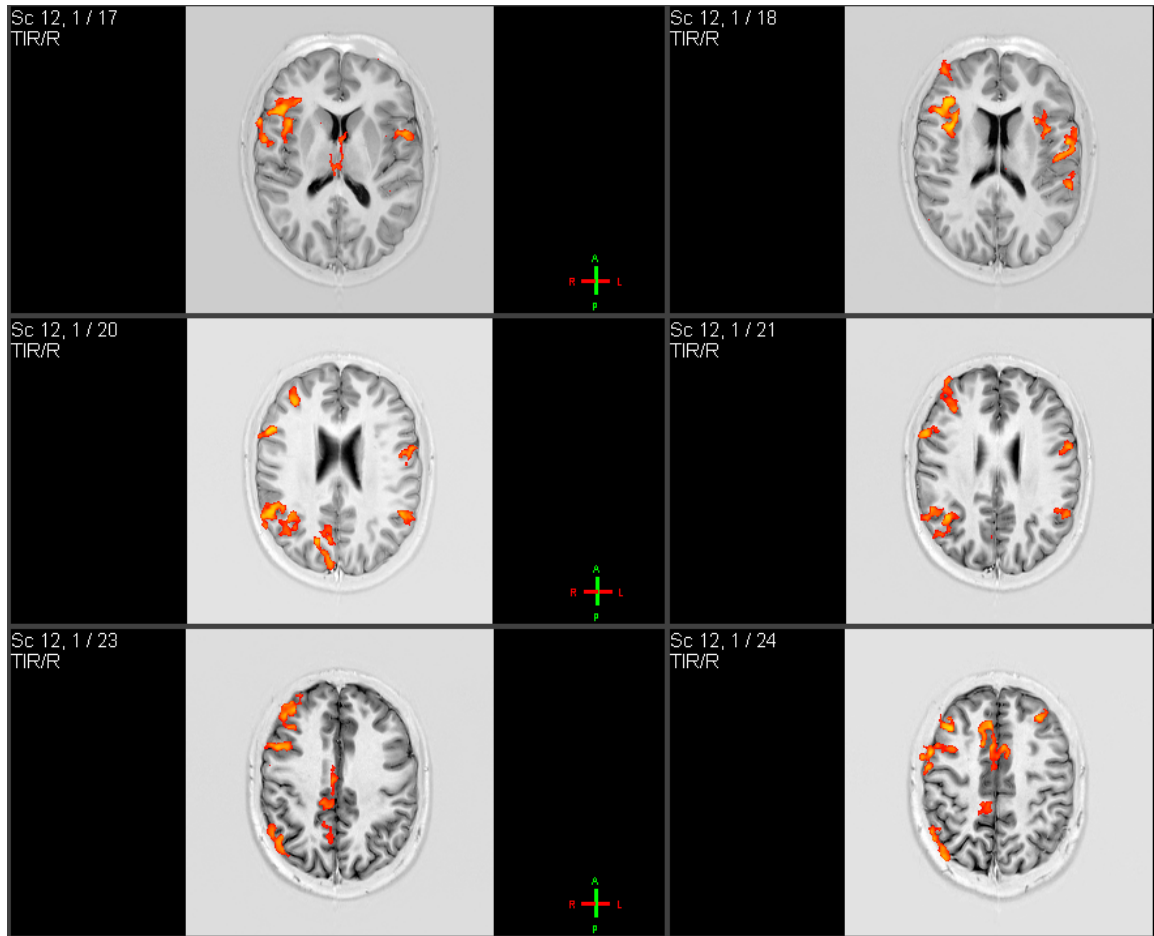


Figure 3.8 Tabasco sauce is very potent and the response from the smell can be seen in regions outside of the limbic system and other areas usually identified as olfactory sites. The red colored areas represent activated regions of the brain.

Along with the change in scents, there was a need to better understand what was causing a decrease in receptor site activation as the scan time was lengthened or repeated frequently. As the time of scent exposure increased or repeated, much of the olfactory response was lost. Activation sites began to decrease as imaging continued. As the

number of cycles was repeated in a single acquisition scan, a saturation or habituation effect was displayed as a loss of activation. It has been shown that adaptation and habituation resulted in decreased response under repeated or prolonged activation (Cerf-Ducastel 2004).

Factors Involving Image Acquisition

Overall time was based principally on the established TR values for the functional acquisition. Each dynamic had a TR of about 3500ms which meant the total scan time lasted approximately five minutes. Shortening the overall total time of the scan meant a decrease in the total amount of scent delivered. The first attempt was to use a total of eight dynamics; the initial background dynamics followed by four activation dynamics. To help compensate for the decrease in the number of dynamics, the TR value was increased to 6000ms, for a total scan time of about 48 seconds. It was determined that 6000ms was too long of a TR period, possibly due to this habituation effect. Ultimately the chosen TR value that gave the best results was 3500ms and a TE as low as possible, usually around 35ms. With an extended TR, such as 6000ms, the saturation effect could be seen. The signal intensity decreased as acquisition time was extended; ultimately leaving very little signal to be observed. With a very short TR value, such as 2000ms, a large amount of noise was observed. The initial signal intensity was more global, probably due to overall increased blood volumes as a result of initial scent delivery, or motion.

Other factors of image acquisition were tested and changed periodically. Slice thickness and slice angle were two of these factors. The thinner the image slices, the

greater the number that is required to cover a given area, which also increases the time. Slices were tested at 2mm, 3mm, and 4mm thicknesses with a final determination that 3mm angled to connect the genu and rostrum of the corpus callosum, provided sufficient anatomical information and functional data. This was in position with the canthomeatal line on most subjects and averaged twenty slices per scan.

There were many instances where it appeared as though the brain was anticipating the induction of a smell (priming effect) at the beginning of each olfactory scan sequence. Figure 3.9 shows regions of the brain with colored ROI's for graphic response analysis, and the relative percent of activation in these regions as a function of time. The graph also demonstrates the alleged priming effect; the initial spike in activity at the start of the scan, even though the scent was not introduced until near the end of the scan.

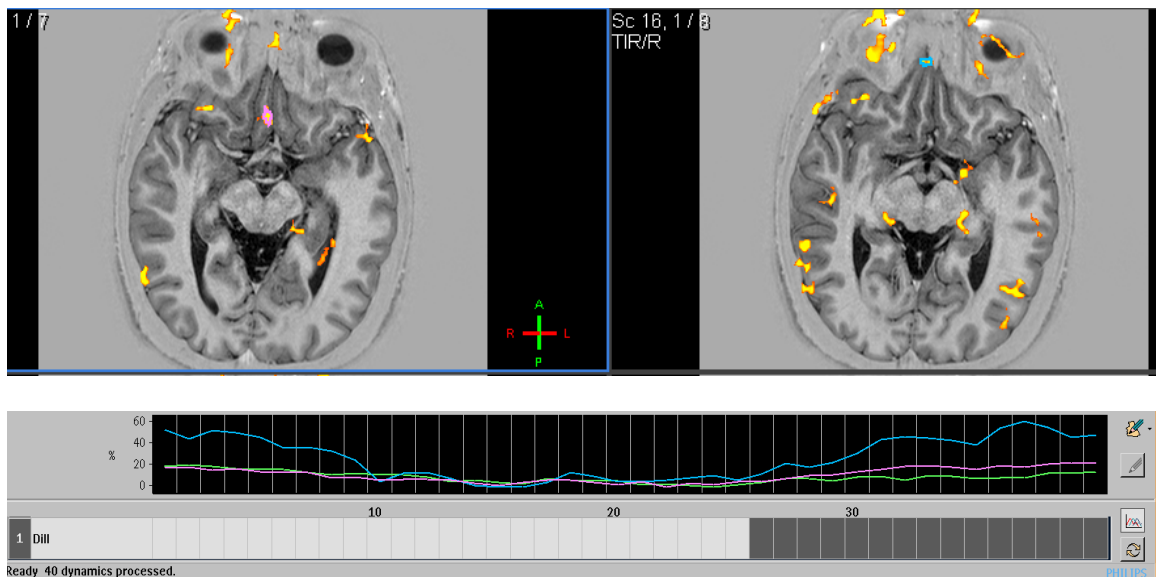


Figure 3.9 Activated brain regions above; some with regional ROI's drawn for analysis. The color of the ROI corresponds with the signal percent versus time curve in the graph below. Notice the initial spike in activity at the beginning of the scan; this has been identified as a priming effect. The priming effect appears to show activation response when there truly was no activation.

Factors Affecting Image Quality

The quality of MRI images can be degraded through the appearance of artifacts. Artifacts can have many causes, and a few were seen with the images acquired. Susceptibility artifacts are those that cause signal loss or field distortion. Signal loss is often caused by tissue-air interfaces. Sinuses and the sinus cavity are common places for these signal-loss artifacts due to the rapid dephasing where tissue and air join together. Another example of a susceptibility artifact is metal. When the protons recess at frequencies different from the Larmor frequency, a field distortion is created (Bushberg 2002). An example of field distortion can be seen in a person wearing a metal retainer on the lower jaw in Fig. 3.10.

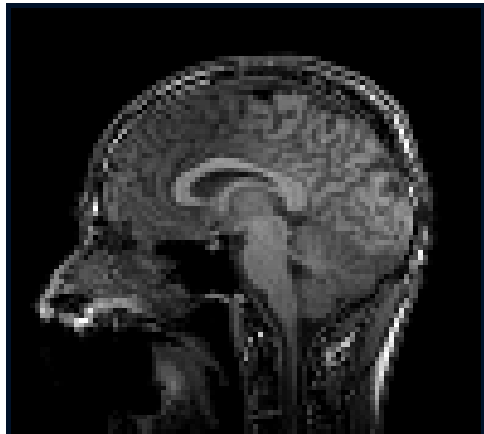


Figure 3.10 an example of the field distortion in a person wearing a metal retainer on the lower teeth. The magnetic field bends around the metal area which therefore does not give off a signal, leaving a black void in the image.

Magnetic field gradients identify the location of excited protons within the brain and spatially encode them. Two common gradient field artifacts that were visualized were the Gibbs phenomenon, and one caused by eddy currents. The Gibbs artifact can be

seen as waves in the image, or alternating lines of signal intensity as in the superior, and posterior aspects of the head in Fig. 3.10 showing a large transition in signal amplitude (Bushberg 2002). Gibbs rings are caused by “insufficient collection of samples in either the phase encoding direction or the readout direction” (Zhuo 2009). It is also noted that the signal has not fully decayed to zero by the end of the acquisition window (Hornak 2009). Ultimately the acquisition matrix is too small; increasing the matrix size can reduce the artifact. Another distortion caused by eddy currents gives the effect of stretching, or wrapping around of the image as in Fig. 3.11. Eddy currents are electric currents induced in a conductor by a changing magnetic field or by motion of the conductor through a magnetic field. It is a source of concern of potential hazard in very high magnetic fields, but it also degrades the overall MR image outcome (Magnetic Resonance 2009).

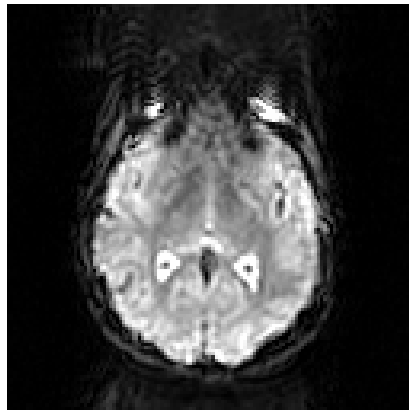


Figure 3.11 a common artifact due to eddy currents shows a stretching of the face, to the point that it appears to be wrapping around to the back of the image. There is also an alternating pattern of signal intensities.

One of the first steps in post-acquisition processing was the creation of a

stimulation protocol in BrainVoyager QX. By creating a stimulation protocol, the computer generates a stimulus time graph that tracks activation based on a given model. In the research of olfaction there was only one stimulus parameter, but in some cases that parameter was introduced multiple times throughout a single scan. These on and off periods were defined as the stimulation protocol to better analyze the activated regions.

Motion was corrected in all three imaging planes as well as rotationally around the x, y, and z axis. An example of a graph showing the extent of motion correction is seen in Fig. 3.12.

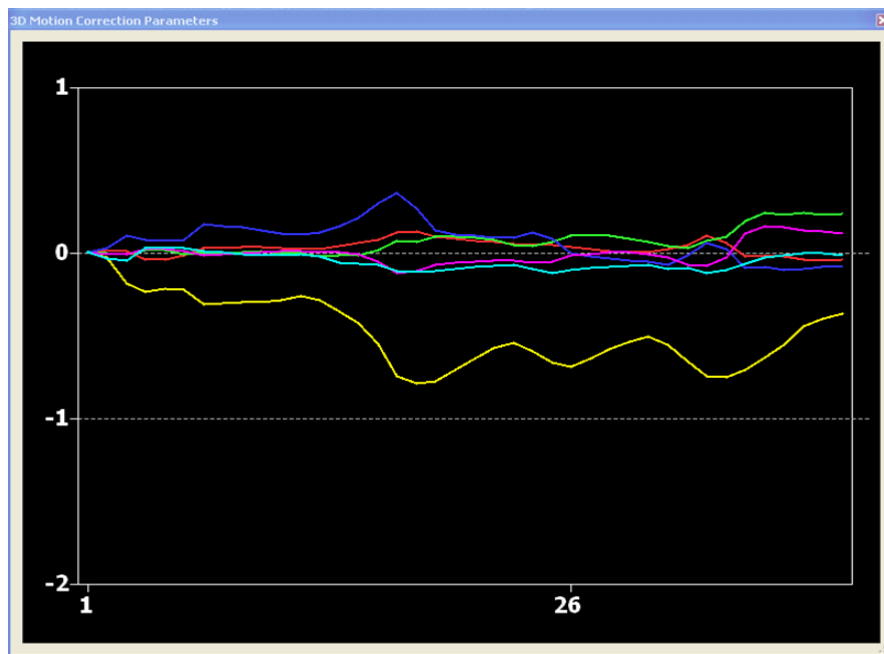


Figure 3.12 Example of a motion correction scheme. Correction takes place for 6 different areas of movement. Red represents translation in the x-direction, Green is translation in the y-direction, Blue is translation in the z-direction, Yellow is rotation around the x-axis, Magenta is rotation around the y-axis, and Cyan is rotation around the z-axis.

The purpose of the stimulation protocol was to graphically represent the

hemodynamic changes within a specific region of activation. An example of this is displayed in a time course plot, and can be seen in Fig. 3.13. The blue represents the off phase where no scent was administered and the red represents the periods in which a scent was given; hence a response was expected. A spike in the red region is favorable. The spikes in Fig. 3.13 do not occur right at the beginning of the stimulated region, because there is a period of hemodynamic delay; the brain has a slight delay due to transit time from the nasal passages to the olfactory receptors. This hemodynamic delay was found to be on the order of three to six seconds in our testing.

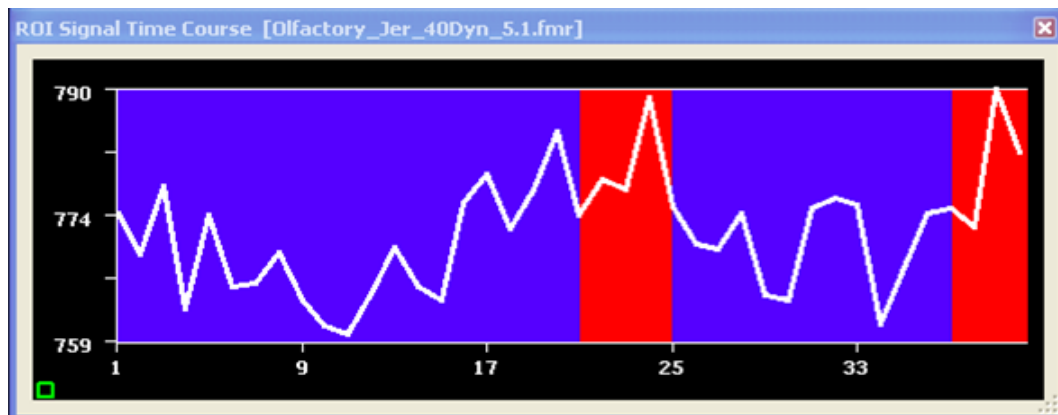


Figure 3.13. This is an example of a Time-Course-Plot showing regional activation throughout the scan duration. The red region represents the “on” phase where a scent was administered. The blue region represents the “off” phase where no scent was given and the patient was left to breathe room air.

The general linear model, or GLM, allowed a specific model to be “fitted” to a time course plot of each voxel resulting in a given value telling how well the chosen model explained the time course (Goebel 2008). Once completed, a statistical t-map was generated showing regions ranging from a dark orange color to a bright yellow. By using the time-course-plots and the GLM overlapping, it was possible to review the statistics of

each region of interest. Figure 3.14 is an example of some of the statistical values this process provides.

ROI Time Course - GLM Results

ANOVA					
Source of Variation	df	SS	MS	F	p
Regression	1	1584.357	1584.357	15.591	0.000171
Residual	78	7926.328	101.620		
Total	79	9510.684	120.388		
data points = 80 R = 0.408 adj.R = 0.395 AR(1) = 0.654					

Figure 3.14. Statistical data returned through GLM analysis on an activated region. The R value on the bottom row of the first ANOVA table gives us an idea of how well the model fits to the data, it is also known as the “multiple correlation coefficient”. A p-value is also generated that tells us the probability that we are seeing what we should expect to see, based on the given predictor.

The last part of the BrainVoyager software that was used for analysis was the anatomical overlay feature. This feature allowed the functional data to be coregistered with anatomical data for more accurate localization of cerebral regions. Once the functional data was coregistered with the anatomical data, coordinate values, as well as p-values, could be recorded. The images display the anatomical regions in all three standard planes; coronal, sagittal, and transverse. Figure 3.15 shows an example of the coregistered image produced with the same activated region visualized in three separate planes. For every marked voxel, there are x, y, and z coordinates given and a p-value.

The p-value for the image set as a whole was recorded, as well as the “multiple correlation coefficient” (R) values, and p-values for selected ROI’s.

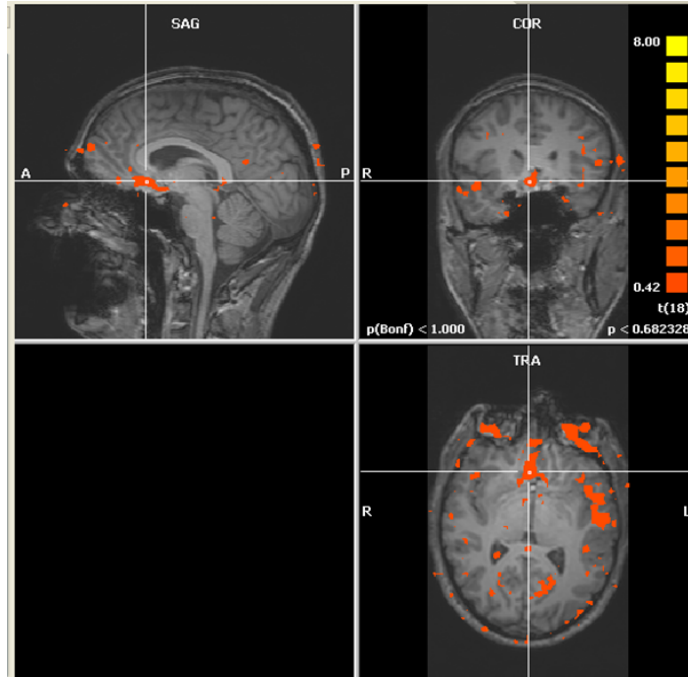


Figure 3.15. This is a coregistered image of functional data with anatomical data. Activated region is isolated with voxel coordinates $x=128$, $y=98$, and $z=134$, localizing the same point in all three planes.

Image Data Results

One hundred seventy eight of the scans that were acquired, had relative acquisition data, and/or observational notes recorded. 54% of all acquired scans ended after the “on” phase, 46% ended following an “off” phase. Twenty one percent of the scans began with scents being administered, while 79% of scans began without scent activation. Seven scans were processed using the BrainVoyager 2.6 for analysis. From these seven processed images, it was noted that a variety of regions within the brain were activated; meaning there was a signal response from cerebral blood flow on the

functional MR acquisition. Some areas of the brain had greater signal response than others, and at varying signal strengths. The data shows inconsistencies in regional cerebral blood flow, which could be due to multiple factors that may include, but are not limited to motion, hardware instabilities, user error, the patient's physical condition, lack of uniformity in choice of scents for processed data, and altered breathing patterns. Other regions showed consistencies for signal strength activation. Many of the images had an excess of noise identified. Noise was considered anything without statistical significance, or where the p-value of the ROI was greater than 0.25.

Inconsistencies were shown throughout the temporal and parietal lobes, thalamus region, regions of the basal ganglia, and the insula. The inconsistencies can be seen in Fig. 3.16. Inconsistencies are classified as those appearing on less than 70% of processed images, yet appearing more than once. Some of these regions are known to have some association with the olfactory processes. These inconsistencies brought to question the validity of signal response as a result solely from olfactory stimulation. This may be due in part to one's ability to recognize certain scents, such as those that are duller versus some that may be stronger or more potent.

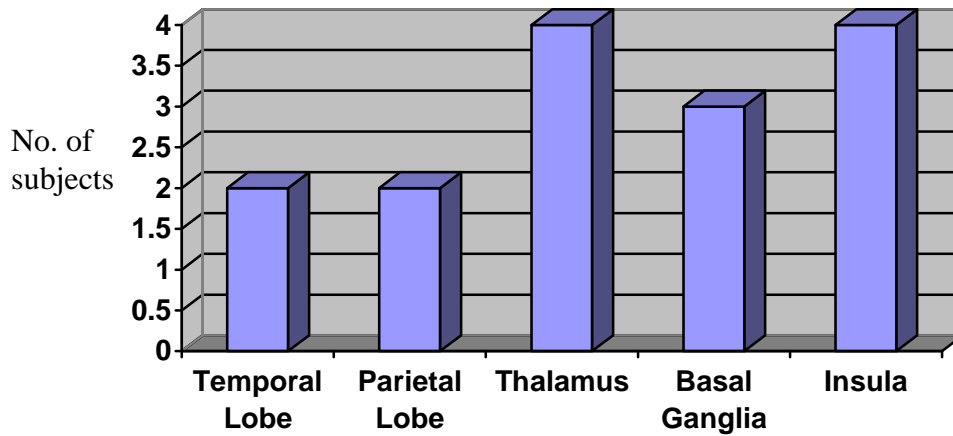


Figure 3.16. Inconsistencies in functional imaging with the use of isopropyl alcohol and dill weed on 7 subjects

The regions of activation that were most consistent on a scan-by-scan basis, regardless of type of scent administered, were located on or near the optic tracts, the orbital regions, frontal lobe, and regions involving parts of the limbic system to include the olfactory tracts. The graphic distribution can be seen in Fig 3.17.

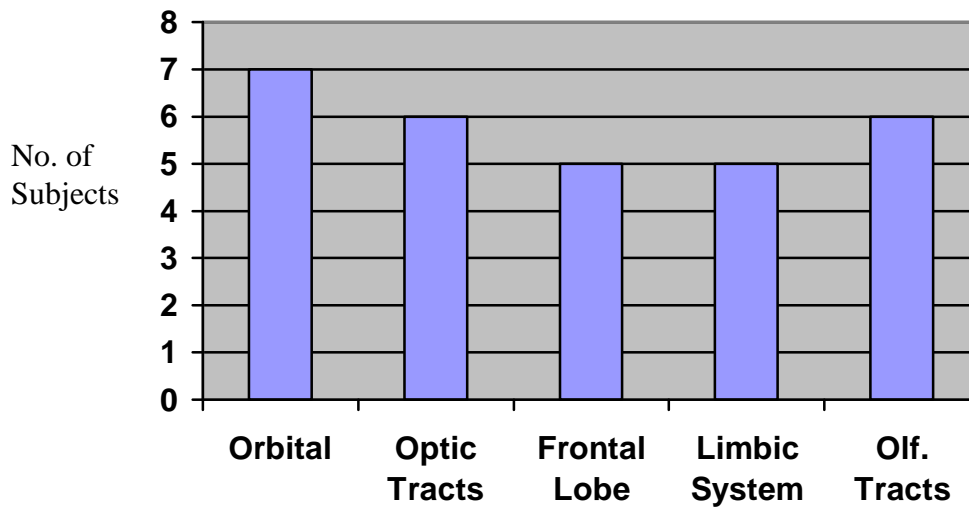


Figure 3.17. Consistencies in functional imaging with the use of isopropyl alcohol and dill weed in 7 subjects

Throughout the observation of receptor site activation, it was concluded that there may be three levels of response from the olfactory process. The primary response centers seem to be within the nasal passages, and olfactory bulb. The secondary receptor regions are contained within the areas of the limbic system that are located at the distal ends of the olfactory tracts. This would include the amygdala, the cingulate gyrus, the hippocampus, and the parahippocampal regions. Observance of signal response in the basal ganglia, to include putamen and caudate nucleus, and insula compose the tertiary regions of olfactory reception. It was again noted that the thalamus could also be considered a tertiary receptor site when imaging with alcohol based products.

CHAPTER 4

DISCUSSION AND CONCLUSION

The aim of the present study was to develop a functional MR protocol for imaging neuronal responses from olfactory stimuli. The results could eventually assist in the diagnosis or staging of early onset Parkinson's disease or other dementias.

Delivery Device

The delivery device used in this research project was a low-budget; cost effective means of delivering aqueous, scented solutions to a subject for the purpose of imaging olfactory receptor sites in the brain. After many prototypes, the open-ended flow circuit aimed in the direction of the nostrils mentioned in chapter 2, Figs. 2.8 and 2.9 was chosen as the best device for use in this research project. The device was compatible with all head sizes and it forced the air directly in front of the nasal passages. It could be mounted temporarily to the coil, or permanently if desired without interference to the coil or its accessories.

Another issue up for debate is when or whether or not to clean or replace the oxygen tubing or scent delivery device. Does the aqueous solution work itself into the matrix of the PVC pieces? Is flushing oxygen tubing with pure oxygen sufficient to remove all traces of the solution, so as to not be detected too early by the next patient? After repeated use of the scent boxes, it was noticed that the scent would linger, even after having washed with soap and water. Replacement pieces would be a must if this kind of device were to be used with greater frequency.

It is not practical in all healthcare settings to have a second technologist to operate the flow of oxygen and alternate the scents being delivered. For research purposes, the system was cost-effective and worked well, and could thus be duplicated easily. If this design were to be implemented on a more permanent basis, it would be advisable to automate the system where it can be controlled by the imaging technologist.

Data Acquisition

The acquisition of functional MRI is achieved by the use of Echo Planar Imaging (EPI). EPI is a method of creating a complete image from a single data sample, or a single “shot” (Cohen 1998). This EPI allows the image acquisition to take place at a fast pace, which improves the quality of the image by limiting the possibility of motion artifacts. While motion artifacts may be limited, EPI has been known to create ghosting and shape distortion artifacts. With Echo Planar Imaging, results are available within seconds of onset of activation with stimulation (Price 2002). When identifying regions of activation, thinner slices are preferred to identify more accurately the anatomical location of the activation. With thinner slices comes a steeper gradient, the steeper the gradient, the more stress introduced which causes an increase in eddy currents. An increase in stress creates a longer recovery time, which in turn creates more ghosting artifacts. To minimize the ghosting, a slice thickness must be chosen that will allow for good anatomical identification while minimizing stress on the gradients.

The physical state of the subject during acquisition could have been regulated differently at various points. Normal breathing patterns cause uncontrolled motion of the body which can travel to the head. Varied breathing cycles also have an impact of the

rate at which the scent is registered by the individual, thus adding statistical variation in the responses. Maintaining a normal breathing cycle is difficult when the person is tired. Breathing patterns are altered as a person relaxes more and more.

Imaging neuronal responses late at night can also decrease the quality of images, because the brain's response time may be slowed. The forced air flow rate being too high also created some discomfort leading to undesired motion, and possible activation sites. Some subjects were sniffing the scent as opposed to just simply inhaling. They were expecting scent, but because the scent was not strong enough for them, they wanted to increase their perception and resorted to sniffing. Sniffing versus inhaling an odorant can make a difference in whether cerebral blood flow changes are solely due to olfactory processing and not motor response (Sobel 1998).

Every person has different levels of smell. While a scent is pleasant to one, it may not be pleasant to another. One item of importance that was not fully taken into consideration with this research was the establishment of a baseline for each individual subject. One way of accomplishing this would have been to perform a University of Pennsylvania Smell Identification Test (UPSIT) or a Connecticut chemosensory test. Both sniff tests aide in identifying or quantifying one's ability to smell. By performing one of these tests prior to image acquisition, a baseline of what scent may or may not be used could have been established. Another option was to have run a placebo scan, or a functional scan without the administration of a scent. Following the placebo scan, the individual with a scent-administered exam and then comparing the two for changes or differences would have also given a sufficient baseline for individual scent recognition.

When the scent was initially delivered, an overall increased blood volume was identified. This is due to a variety of factors to include; initial scent recognition, and possible head or visual motion as a response to the introduction to the scent. Stability of the patient is important. The patient should not move or distort more than a pixel during the image acquisition phase. Patient motion can be caused by instability of the radiofrequency transmitter, gradient and shim hardware, and the patient's ability to remain motionless (Price 2002). Processing software can correct for some motion occurring during acquisition, but the question arises whether or not that motion correction is correcting the BOLD response as well or just the image quality of the brain. Motion correction of this kind does not completely remove the effects of movement upon the BOLD fMRI signal, because movement within the field gradients during scanning alters the signal contained at different points during the slice acquisition. Even after realignment of the brain to its original position, movement-induced signal artifacts can remain (Faro 2006).

Data Processing

The use of the IViewBold application on the acquisition computer proved to be a good tool to judge generally if a response was recognized or not. Based on the images viewed during "real-time" imaging, some changes in scan time, length of scent administration, and quality of the scent could be altered, and without getting the patient out of the scanner, the subject could be re-imaged. The anatomical scan can be overlaid to try and identify activated regions. These images were based entirely off of the data acquired from the immediate scan without any type of image alteration. Applying a

motion correction factor was needed in most cases, because of the nature of the scan, the signal strength of the radiofrequency pulses, and the patient's normal breathing patterns.

Motion correction and image analysis was performed using BrainVoyager software. The image quality and slice data from the processing software was valuable, but the time required to process a single study made the course tedious and unwelcoming. Anatomy verification in X, Y, and Z planes was not as accurate as it could have been. The patient position varied from scan to scan. No fiducial markers were used to verify the repeat placement of the patient for repeat scanning. X, Y, and Z coordinates were used to verify location of activated regions on a single scan, but were unacceptable when it came to intrapatient comparisons because of the changes in head or body placement.

Different Scent Responses

Some scents that were used created varied and unexpected results. While it is known that the thalamus is the gateway to the cerebral cortex and plays a role in organizing and distributing received sensory information (Marieb 2001), it is unclear why alcohol had a tendency to demonstrate increased signal intensity in this region when compared with other scents. Another extreme case was that of the administration of tabasco sauce. This caused an overall increase in signal intensity and activated regions. These regions extended up to the longitudinal fissure and were identified bilaterally right to left as well as anterior to posterior. Because tabasco sauce is such a potent or unpleasant smell for most people, it is theorized that other regions are activated based on, motion of head, body, or eyes, and maybe even memories of previous experiences.

Excessive exposure to a scent caused a decrease in the number of activation sites and a decrease in signal intensity of individual sites. An example would be that of a 10 dynamic exposure sequence which would allow scent exposure non-stop for more than thirty seconds. It is hypothesized that this is due to a saturation of the receptors; they became overloaded and were unable to register any new scent.

As the number of cycles was repeated in a single acquisition scan, a saturation effect was evident. Some possible factors included the duration of the total fMR scan, the length of the TR used, or even the length of the “on-phase” of the dynamics, or the time during which the scent was administered.

Conclusion

The creation of an olfactory protocol for functional MR imaging requires much attention to great detail. Some of these details include: patient position and placement in the scanner, the establishment of an individual baseline test for patient response comparison, the type of scent administered and the flow rate and location of air delivery to the patient. Other fine details include the length of each scan, the positioning of slices that are being acquired, and the monitoring of breathing patterns and motion. A small TR value between 2000ms and 3500ms seems to give the best BOLD response from the fast blood flow through veins. This signal response can be overlaid on an anatomical data set to identify locations throughout the brain where olfaction is being processed. Too much of a scent has been determined to habituate or saturate the cells and therefore must be limited to no more than two cycles throughout the functional acquisition. There must also be a delay time between scent administrations of about 3.5 times the administration

period. This allows time for the odor to exit the cells.

This research verified, that the olfactory regions can be identified utilizing fMRI, however, changes in olfactory response were statistically not measureable. Refinement of the analyses techniques can allow clinicians to (1) determine an average age specific olfactory response to various scents and (2) determine if patients present with responses that are statistically abnormal.

This protocol development opens doors to new opportunities for research in neurological sciences. As the average age of the population increases and as there is a greater increase in persons with dementia, there is a need to better understand and prepare for these life changing conditions. By performing olfactory response on those who have a strong genetic predisposition for Alzheimer's or Parkinson's disease, families can better prepare mentally, physically, and emotionally. For many who struggle with epilepsy, and may require surgical procedures as the only means of a cure, functional MRI can help surgeons and other physicians know what kind of long term effects may result from such procedures. If one is to lose the ability to smell, the sense of taste is greatly inhibited also, which can cause some drastic lifestyle changes.

Functional MRI is a relatively safe method of helping determine brain function capabilities, and the extent of neurological damage. The Olfactory process is a sophisticated one that involves multiple response centers within the brain. Isolation of the response areas can be achieved for olfaction as well as other areas of the brain. Identification and localization will continue to improve as technology and computers become more advanced. There are still many roads to be taken; as for this one, it was the one less traveled.

REFERENCES

- Bohnen NI, Gedela S, Kuwabara H, Constantine GM, Mathis CA, Studenski SA, Moore RY. Selective Hyposmia and Nigrostriatal Dopaminergic Denervation in Parkinson's Disease. *Journal of Neurology* 254:84-90; 2007.
- Brand G. Olfactory/trigeminal interaction in nasal chemoreception. *Neuroscience and Behavioral Reviews* 30: 908-917; Jan. 2006.
- Bushberg JT. *The Essential Physics of Medical Imaging*. 2nd ed. Philadelphia: Lippincott Williams & Wilkins; 2002.
- Bushong SC. *Magnetic Resonance Imaging: Physical and Biological Principles*. 3rd ed. Missouri: Mosby, Inc; 2003.
- Cerf-Ducastel, B, and Murphy, C. Improvement of fMRI data processing of olfactory responses with a perception-based template. *NeuroImage* 22: 603-610; 2004.
- Children's HL (Children's Health Library). University of Chicago Comer Children's Hospital Children's Health Library Glossary. Available at: <http://www.uchicagokidshospital.org/online-library/content=P02036#T>. Accessed 19 Nov. 2007.
- Cohen, Mark. Echo-planar imaging (EPI) and functional MRI. PA Bandetti and C Moonen. 1998. Accessed online and available at: http://airto.hosted.ats.ucla.edu/BMCweb/BMC_BIOS/MarkCohen/Papers/EPI-fMRI.html.
- CPME: International Center for Postgraduate Medical Education. MRI For Technologists. Module 1: Basic Principles of MRI. USA: Berlex Laboratories; 2001.
- Crimando, J. "Cranial Nerves: Review Info." Bio201 Gateway Community College. Available at: <http://www.gwc.maricopa.edu/class/bio201/cn/cranial.htm>. Accessed 18 Nov. 2007.
- De Kruijk JR, Leffers P, Menheere PPCA, Meerhoff S, Rutten J, Twijnstra A. Olfactory function after mild traumatic brain injury. *Brain Injury* 17:73-78; 2003.
- Encyclopædia Britannica. Encyclopædia Britannica Online word search, smell [Online]. Available at: <http://www.britannica.com/eb/article-9068254>. Accessed 20 Nov. 2007.
- Faro SH, Mohamed FB Eds. *Functional MRI: Basic Principles and Clinical Applications*. New York, NY. 2006.

- Fontanini A, Bower JM. Slow-waves in the olfactory system: an olfactory perspective on cortical rhythms. *Trends in Neuroscience* 29(8): 429-437; July 2006.
- Frahm J, Merboldt K-D, Hanicke W, Kleinschmidt A, Boecker H. Brain or vein-oxygenation or flow? On signal physiology in functional MRI of human brain activation. *NMR in Biomed* 74:229-243; 1994.
- Garcia-Falgueras A, Junque C, Jiménez M, Caldu X, Segovia S, Guillamon A. Sex differences in the human olfactory system. *Brain Research* 1116: 102-111; 2006.
- Glowniak JV, Zak I. Available at: "The Limbic System". Wayne State University. http://www.med.wayne.edu/diagradiology/Limbic%20System%20RSNA%202004/Home_Page.html. Accessed 23 Jun. 2008.
- Goebel R, Jansma H, Seitz J, Heinecke A. *Brain Voyager QX Getting Started Guide*. Version 2.6. 2008.
- Gomot M, Bernard FA, Davis MH, Belmont MK, Ashwin C, Bullmore ET, Baron-Cohen S. Change detection in children with autism: an auditory event-related fMRI study. *NeuroImage* 29: 475-484; 2006.
- Gonzalez J, Barros-Loscertales A, Pulvermuller F, Meseguer V, Sanjuan A, Belloch V, Avila C. Reading Cinnamon Activates Olfactory Brain Regions. *NeuroImage* 32:906-912; 2006
- Green P, Rohling ML, Iverson GL, Gervais RO. Relationships between olfactory discrimination and head injury severity. *Brain Injury* 17(6): 479-496; (2003).
- Hendee WR, Ritenour ER. *Medical Imaging Physics*. 4th ed. New York: Wiley-Liss, Inc: 2002.
- Hornak, Joseph P. *The Basics of MRI*. 1996-2009. available at: <http://www.cis.rit.edu/htbooks/mri/chap-11/chap-11.htm#11.11>. Accessed 15 Nov 2009.
- Huttenbrink, K.B. Disorders of the Sense and Smell of Taste. *Ther Umsch* 52(11): 732-737; November 1995.
- Iannilli E, Gerber J, Frasnelli J, Hummel T. Itranasal trigeminal function in subjects with and without an intact sense of smell. *Brain Research* 1139: 235-244; Jan. 2007.
- Jacob, Tim, comp. *Smell (Olfaction) a tutorial on the sense of smell*. Cardiff University, UK [online]. Available at: <http://www.cf.ac.uk/biosi/staffinfo/jacob/teaching/sensory/olfact1.html#receptor>. Accessed 18 Nov. 2008.

- Kamitani Y, Tong F. Decoding the visual and subjective contents of the human brain. *Nat Neuroscience* 8(5): 679-685; May 2005.
- Killgore WDS, McBride SA. Odor identification accuracy declines following 24 Hour Sleep Deprivation. *Journal of Sleep Research* 15(2): 111-116; June 2006.
- Kim, S-G, Ugurbil, K. Functional magnetic resonance imaging of the human brain. *Journal of Neuroscience Methods* 74:229-243; 1997.
- Leffingwell, John C. "Olfaction - a Review." Leffingwell and Associates [online]. Available at: <http://www.leffingwell.com/olfaction.htm>. Accessed 18 Nov. 2007.
- Liu T, Pestilli F, Carrasco M. Transient Attention Enhances Perceptual Performance and fMRI Response in Human Visual Cortex. *Neuron* 45:469-477; Feb 2005.
- Lledo P-M, Gheusi G, Vincent J-D. Information processing in the mammalian olfactory system. *Physiological Reviews* 85:281-317; 2005.
- Machielsen WCM, Rombouts SAR, Barkhof F, Scheltens P, Witter MP. fMRI of visual encoding: Reproducibility of Activation. *Human Brain Mapping* 19:156-164; 2000.
- Magnetic Resonance - Technology Information Portal. "Eddy Currents". Available at: <http://www.mr-tip.com/serv1.php?type=db1&db=Eddy%20Currents>. Accessed 30 Aug 2009.
- Marieb EN, Eds. *Human Anatomy and Physiology*. 5th Ed. Benjamin Cummings, 2001. 561-564.
- Marx E., Stephan T., Deutschlander A., Seelos K.C., Dieterich M., Brandt T. Eye closure in Darkness Animates Sensory Systems. *Neuroimage* 19: 924-934; 2003.
- Marx E., Deutschlander A., Stephan T., Dieterich M., Wiesmann M., Brandt T., Eyes opened and eyes closed as rest conditions: impact on brain activation patterns. *Neuroimage* 21: 1818-1824; 2004.
- Menon R, Kim S-G. Spatial and temporal limits in cognitive neuroimaging with fMRI. *Trends in Cognitive Science* 3:207-215; 1999.
- Mueller A, Abolmaali ND, Hakimi AR, Gloeckler T, Herting B, Reichmann H, Hummel T. Olfactory Bulb Volume in Patients with Idiopathic Parkinson's disease – a Pilot Study. *Journal of Neural Transmission* 112(10):1363-1370; Oct. 2005.
- Murphy C, Cerf-Ducastel B, Calhoun-Haney R, Gilbert PE, Ferdon S. ERP, fMRI and functional connectivity studies of brain response to odor in normal aging and Alzheimer's disease. *Chemical senses* 30(1):170-171; 2005.

- NYAS. New York Academy of Sciences: About the Academy. Available at: <https://nyas.org/about/newsDetails.asp?newsID=65>. Accessed 22 Nov 2007.
- Price RR, Allison J, Massoth RJ, Clarke GD, Drost DJ. Practical aspects of functional MRI (NMR Task Group #8). *Medical Physics* 29(8): 1892-1912; August 2002.
- Roy CS, Sherrington CS. On the Regulation of the Blood Supply of the Brain. *J. Physiology* 11(1-2):85-108; Jan. 1890.
- Rozin P. Taste-smell confusions and the duality of the olfactory sense. *Perception & Psychophysics* 31:397-401; 1982.
- Sabri M, Radnovich AJ, Li TQ, Kareken DA. Neural correlates of olfaction change detection. *NeuroImage* 25:969-974; Feb. 2005.
- Schafer JR, Kida I, Xu F, Rothman DL, Hyder F. Reproducibility of odor maps by fMRI in rodents. *NeuroImage* 31:1238-1246; Apr. 2006.
- Schild HH. *MRI Made Easy*. 1992. Wayne, NJ: Berlex laboratories, 1994.
- Shepherd GM. Outline of a theory of olfactory processing and its relevance to humans. *Chemical senses* 30(1):i3-i5; 2005.
- Shepherd GM. Smell images and the flavour system in the human brain. *Nature* 444:316-321; Nov. 2006.
- Sobel N, Prabhakaran V, Desmond JE, Glover GH, Goode RL, Sullivan EV, Gabrieli JD. Sniffing and Smelling: Separate Subsystems in the Human Olfactory Cortex. *Nature* 392:282-286; 19 Mar. 1998.
- Sommer U, Hummel T, Cormann K, Mueller A, Frasnelli J, Kropp J, Reichmann H. Detection of Presymptomatic Parkinson's Disease: Combining Smell Tests, Transcranial Sonography, and SPECT. *Movement Disorders* 9(10):1196-1202; May 2004.
- Stocker T, Keller T, Schneider F, Habel U, Amunts K, Peiperhoff P, Zilles K, Shah NJ. Dependence of Amygdala Activation on Echo Time: Results from Olfactory fMRI Experiments. *NeuroImage* 30:151-159; Nov. 2005.
- Tolosa E, Wenning G, Poewe W. The Diagnosis of Parkinson's Disease. *Lancet Neural* 5:75-86; Jan. 2006.
- Truwit CL, Lempert TE. *High Resolution Atlas of Cranial Neuroanatomy*. Baltimore, MD: Williams & Wilkins, 1994.

- Villemune C, Wassimi S, Bennett GJ, Shir Y, Bushnell MC. Unpleasant Odors Increase Pain Processing in a Patient with Neuropathic Pain: Psychophysical and fMRI investigation. *Pain*. 120(1/2):213-220; Jan. 2006.
- Vokshoor A, McGregor J. Anatomy of Olfactory System. *Emedicine.Com*. Available at: <http://www.emedicine.com/ent/topic564.htm>. Accessed 18 Nov. 2007.
- Voron SC, Stensaas SS. HyperBrain Syllabus Chapter 1. HyperBrain [online]. University of Utah School of Medicine. Available at: <http://library.med.utah.edu/kw/hyperbrain/syllabus/syllabus1.html>. Accessed 19 Nov. 2007.
- Whitfield P, Stoddard DM. *Hearing, Taste, and Smell; Pathways of Perception*. New York, NY: Torstar Books, Inc., 1984.
- Wiesmann M, Kopietz R, Albrecht J, Linn J, Reime U, Kara E, Pollatos O, Sakar V, Anzinger A, Fesl G, Bruckmann H, Kobal G, Stephan T. Eye closure in darkness animates olfactory and gustatory cortical areas. *NeuroImage* 32:293-300; May 2006.
- Zhuo J, Gullapalli RP. MR Artifacts, Safety, and Quality Control. *RadioGraphics* 26:275-297; Jan 2006. Available online at: <http://radiographics.rsna.org/content/26/1/275.full>. Accessed 15 Nov 2009.

APPENDICES

Appendix A. A Step-by-step Guide to Image Acquisition Using Philips Intera Software and Philips IViewBold Software Version 1.5.

- 1) Acquiring an olfactory fMRI
 - a) A new exam needs to be created
 - i) Select “Patient”
 - ii) Choose “New Exam”
 - (1) Type data
 - (a) Patient name
 - (b) Registration ID
 - (c) Date of birth (DOB)
 - (d) Exam name
 - (e) Date of exam
 - (f) Patient’s weight
 - (g) Any comments if desired
 - (2) Click on “Proceed”
 - b) Exam type needs to be selected
 - i) A series of tabbed parameter folders appear on bottom right of screen
 - (1) Select the one entitled “Hospital”
 - (2) Select “UNLV/Philips”
 - (3) Select “UNLV”
 - (4) Select “OLF NEW”
 - (5) Select the exam card

- (a) Lt click and drag to the window on the left of the parameter files
- (b) Exams within this folder should appear in a listed format, including:
 - (i) SMARTBRAIN
 - (ii) SENSE Head
 - (iii) T1WRef-fMRI
 - (iv) Olfactory (this is the functional scan)
 - (v) T1W/3D/Sag (this is the anatomical data)
- c) Verify scan parameters
 - i) Lt click on SMARTBRAIN (this is a scoutview of the brain)
 - (1) Verify coil type (8-channel)
 - (2) May have to verify or select anatomical region (brain)
 - (3) Click on “Proceed”
 - ii) Double click on SENSE when scoutview has completed
 - (1) Position the slice markers on the sagittal view (center near the pons of the midbrain, and angled with the genu and rostrum of the corpus callosum)
 - (2) Click on proceed
 - iii) Double-click on Ref_fMRI scan when SENSE has completed
 - (1) Verify information and parameters
 - (a) Slice gap = 0.5
 - (b) Thickness = 3mm
 - (c) Number of slices = 20
 - (2) Click “Proceed”
 - iv) Double click on Olfactory once reference image has started acquiring

- (1) Verify information matches the Ref_fMRI scan
 - (a) TR value = 3500ms
 - (b) TE value = 35ms
 - (c) 20 slices at 30mm thickness
- (2) Click on the “change screen” icon found in the upper left portion of the screen [appears as a half circle (right hemisphere) with a right and left arrow within the hemisphere]
- (3) At the top of the screen, select “Analysis”
 - (a) Select “IViewBold”
 - (b) The toolbar above now has a new “IViewBold” option next to “analysis”. Select this new “IViewBold” option
 - (c) Select desired paradigm
 - (i) Click on Olf 60
 - (ii) Click “OK”
- (4) Left click on the icon with a human stick figure (left middle of screen)
 - (a) Click “Proceed”
 - (b) A window will appear that reads “Waiting to start”. Verify that the person in control of scent delivery is in place and ready
 - (c) Click “Proceed”
 - (d) Once the exam begins, click on the “Change screens” icon again
 - (e) A blue line marker will move across the bottom of the screen on the paradigm or block diagram. When the line arrives at the first gray block, give thumbs up signal to initiate scent delivery. Signal to the

delivery person to change scents on every two blocks, and then to shut off scent when line passes through the final gray box.

(f) Continue as needed until scan is complete

v) Double click on 3D/Sag file (anatomical)

(1) Verify slice placement and orientation

(2) Verify FOV = 256 and Recon = 256

(3) Click on "Proceed"

vi) Once anatomical scan has completed, the total scan acquisition is complete.

Total time is estimated at about 12 minutes

Appendix B. Step-by-step Guide to Processing Olfactory fMRI With *.par and *.rec Files Using Philips' BrainVoyager QX, Version 2.6.

- 1) Processing a brain for analysis with BrainVoyager QX, version 2.6
 - a) A new project is to be created
 - i) After opening the software, click on "file"
 - ii) Select "Create Project Wizard" from the drop-down menu
 - iii) When ready to begin, select "Next"
 - iv) Select the project type: "FMR project" and click on "Next"
 - v) Select "PHILIPS_REC" from the menu and click on "Next"
 - vi) Label the project name for the study. Click on "Browse"
 - vii) Search through the files until finding the functional *.rec file to analyze
 - viii) Double click on the file, or highlight the file and click on "Open".
 - ix) Verify all exam information that is displayed to the left of the screen.
 - x) If this is the correct exam, click on "Next"
 - xi) Verify the correct number of slices and click "Next"
 - xii) Verify the number of volumes (dynamics) in the acquisition
 - xiii) Enter the number of volumes to skip, set at zero if not skipping any.
 1. Note that the 2 dummy scans heard while acquiring are not included in the original count.
 - xiv) Once all information is verified and correct, click on "Next"
 - xv) The last summary page is displayed; if all is good, click "Finish"
 - xvi) A brain image pops up and all data is being submitted

xvii) Once all data is submitted a window will pop up. Check the “verified” boxes (a total of 2), then select “Closed”

2) Creating the stimulation protocol files

- a) Left click on “Analysis” and select “Stimulation Protocol. . .”
- b) Type in a name for the experiment
- c) Left click on “Add” to identify the condition
- d) Highlight the condition and click on “Edit Label”
- e) Type in “on” for that condition and click “OK”
- f) Left click on “Edit Color” and select desired color (red), click “OK”
- g) Click on “Add” again for the “off” condition
- h) Highlight the condition and click on “Edit Label”
- i) Type in “off” for that condition and click “OK”
- j) Left click on “Edit Color” and select desired color (Blue), click “OK”
- k) Left click on “Intervals >>”
- l) Highlight the “on” condition and click on “Add” under the intervals icon
 - i) NOTE: If there are 2 or more “on” intervals, click “Add” for each one
- m) Type in the number of dynamics that fit that condition
 - i) Example: if dynamics 1-10 were “on” during the acquisition, type “1” in the “From” box and type “10” in the “To” box. If another “on” segment was from dynamics 32-38, then those numbers would be typed in under the same place, but categorized as “NrOfIntervals” number “2”.
- n) Highlight the “off” condition and click on “Add” under the intervals icon
 - i) NOTE: If there are 2 or more “off” intervals, click “Add” for each one

- o) Type in the number of dynamics that fit that condition
 - i) Example: if dynamics 11-20 were “off” during the acquisition, type “11” in the “From” box and type “20” in the “To” box. If another “off” segment was from dynamics 22-31, then those numbers would be typed in under the same place, but categorized as “NrOfIntervals” number “2”.
 - p) Left click on “Show Plot” to visualize the dynamic set just created. Make adjustments as necessary to match the acquisition protocol.
 - q) Left click on “Save .PRT...” and type in a file name, then click “Save”
 - r) Go to the top of the window and click “File” and select “Save”
 - s) On the stimulation protocol window it should have “OK” next to the words “Stimulation Protocol” – if this is the case, click “Close”
- 3) Preprocessing of fMR projects
- a) Left click on “Analysis” and select “FMR Data preprocessing. . . “
 - b) Left click in the “Spatial Smoothing” square and select “Go”
 - i) NOTE: the last 4 of 5 items should be selected
 - c) Slice scan corrections will now take place
 - d) When complete, a Motion Correction parameters window will remain open
 - e) Close out the motion correction window by clicking on the “x” in top right corner
- 4) Statistical analysis with the General Linear Model (GLM)
- a) Choose “Analysis” from the menu and select “General Linear Model: Single Study. . .”
 - b) Right click in the red region (the “on” region) and left click on “HRF”
 - c) Click on the “Save. . .” button

- d) Type in a file name to include the phrase “Design matrix” (saves as *.sdm file)
 - e) Left click on “GO”
 - f) Voxel beta plot appears, Close out Beta Plot, and FMR Properties windows
 - g) Adjust threshold values with icons on the Left of the brain slices(they are the 4th and 5th icons from the bottom)
 - h) Left click on “Analysis” and select “Overlay Volume Maps. . .”
 - i) Left click on the “Show Negative” box, removing the checkmark and click “OK”.
NOTE: this is also where cluster sizes can be adjusted to clean up the image
 - j) Adjust the matrix display as desired by Left clicking on the grid icons to the Left of the brain slices, immediately above the threshold icons.
 - k) Left click on “Analysis” from the menu and select “General Linear Model: Single Study. . .”
 - l) Left click in the square next to the number 1 (on) until a “+” sign appears.
 - m) Left click in the square next to the number 2 (off) until a “-“ sign appears
 - n) Left click on “Save .GLM. . .” and name the file (file saved as a *.glm file)
- 5) Detailed GLM analysis of ROI’s
- a) Locate a region in red to analyze. Left click and drag, creating a rectangle over the desired area (creates ROI)
 - i) NOTE: Signal time course plot automatically pops up
 - b) Right click in Signal Time Course window, and select “Show/hide options”
 - c) When expanded window pops up, click on “ROI GLM...”
 - d) Click “Browse. . .”
 - e) Choose the file with the “Designmatrix.sdm” in the title, click “Open” and then

click “Fit GLM”

- i) 1st window shows Signal Time Course
- ii) 2nd Window shows tables with statistical values (multiple correlation coefficient, R, closer to 1.0 means model fits data very well)
- iii) 3rd window shows graphical representation of the data (Blue), the model (Green), and the residuals (red – subtracts the model from the data)

6) Creation of a 3-D anatomical *.vmr file

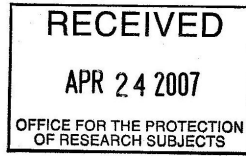
- a) Choose “File” and select “New Project”
- b) Select “Anatomical 3D data set (VMR)” make sure the “File Type:” says “PHILIPS_REC”
- c) Left click on “Select First Source File. . .”
- d) Choose the correct *.rec anatomical file and click “Open” then click “GO”
- e) Allow processing to complete and Adjust contrast if desired, then click “OK”
- f) Type in a file name (will be a .vmr file) and the “Save”
- g) When asked to transform to standard convention, click “Yes” then click “Save” if newly created file is under the correct file folder
- h) Transformation will occur, if an ERROR is created, click “OK”
- i) At the top, click on “File” and select “VMR properties”
- j) Click “Options”, then change all x, y, and z dimension data in bottom row to 256, then click “Frame”
- k) Click “Save” (if asked to replace and overwrite, click “yes”), then click “OK” on the VMR Properties window

7) Coregistration of anatomical and fMR data sets

- a) On the “3D Volume Tools” window click on “Full Dialog>>”
- b) Under “FMR-VMR Coregistration”, left click on “Select FMR. . .”
- c) Choose the longest *.fmr file and click “Open”
- d) Under “FMR-VMR Coregistration”, left click on “Align. . .”
 - i) NOTE: 2 new files are created for “initial alignment” (IA) and for “Final Alignment” (FA)
- e) Select file “Source Options”, check the “Create edge display box” to remove the checkmark, and choose “GO”
- f) After alignment takes place, click on the “Spatial Transf” tab
- g) Click on “Save .TRF. . .” icon
- h) Select the long *.trf file that contains “SAG_FA.trf” at the end and click “Save”
- i) From the top menu, click on “Analysis” and choose “Create 3D-Aligned Time Course (VTC) Data. . .”
- j) Click 1st “Browse. . .” icon and then choose longest *.fmr file, then click “Open”
- k) Click on “Auto-Fill”, then “GO”
- l) When the box asks to continue if data will not be in Talairach space, click “Yes”
- m) When computation completes, close out small black “x” in top right corner
- n) Click on “File” and select “Open. . .” Then choose the “SAG.vmr” file and click “Open”
- o) Click on “Analysis” and choose “Link 3D Time Course (VTC) Data”
- p) Left click on “Browse. . .”
- q) Go to the file folder that contains the *.vtc file and click on it, then click “Open”
- r) Click “OK”

- 8) Loading a GLM on a *.vmr project
 - a) Select “Analysis” and choose “General Linear Model: Single Study. . .”
 - b) Left click on “Load. . .” and select the “. . .autosave.rtc” file and click “Open”
 - c) Left click on “Options. . .” and check the box “Correct serial correlations”
 - d) Click “OK” and then click “GO”
 - e) Close the “Voxel beta plot” window and adjust thresholds as before
 - f) Click on “Analysis” and choose “Overlay Volume maps. . .”
 - g) Uncheck the “Negative” box and click “Close”
 - h) Move the cursor over the anatomy to locate activated regions
 - i) Moving the cursor will give coordinates in x, y, and z planes
 - i) When a desired region is located, record the x,y,and z coordinates
 - j) Right click on that region and choose “Show/hide options”
 - k) When expanded window pops up, click on “ROI GLM...” then click “Browse”
 - l) Choose the file with the “Designmatrix.sdm” in the title, click “Open” and then click “Fit GLM”
 - i) 1st window shows Signal Time Course
 - ii) 2nd Window shows tables with statistical values. Record the R and p-values
 - iii) 3rd window shows graphical representation of the data
 - m) Exit the program when finished

Appendix C: Patient Consent Forms and IRB Approval



TITLE OF STUDY: Investigation of the Reproducibility of Functional Magnetic Resonance Imaging and Diffusion Tensor Imaging.

INVESTIGATOR(S): Jeremy Mangum, Phillip Patton

CONTACT PHONE NUMBER: 702-895-3555 (Phillip Patton), 702-453-4393 (Jeremy Mangum)

Purpose of the Study

You are invited to participate in a research study. The purpose of this study is to test the reproducibility of functional Magnetic Resonance Imaging (MRI) and Diffusion Tensor Imaging MRI in mapping responses of neurological fibers throughout the brain. Both of these procedures are MRI based brain scans that are similar or identical to other MRI procedures.

Participants

You are being asked to participate in the study because we need non-pregnant subjects who are over the age of eighteen willing and available to be imaged five different times in a closed MRI scanner over a given period of time.

Procedures

If you volunteer to participate in this study, you will be asked to do the following: Remain still while lying on an MRI scanning table. A special helmet called a brain coil will be placed over your head for imaging purposes. You may be required to tap your fingers, listen to different noises, or smell different odors on a given command. None of these procedures differ from procedures currently used clinically.

Benefits of Participation

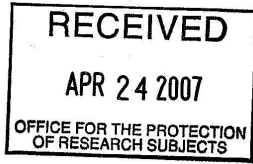
There *may/may not* be direct benefits to you as a participant in this study. However, we hope to learn more about the ability of the brain to reproduce responses to different stimuli and to visualize the appearance of neuron tracts within the brain.

Risks of Participation

There are risks involved in all research studies. This study includes only minimal risks. *There is a risk of falling off the scanner table if not climbing on or off carefully, and there is a risk of claustrophobia, because you will be in an enclosed MRI scanner with a specialized helmet, or coil.* To minimize the risk of falling all subjects will be helped on and off the imaging table. Additionally, all subjects will be monitored during the imaging process via video camera.

Cost/Compensation

There *will not* be financial cost to you to participate in this study other than the cost of travel to and from the imaging center. The study will take approximately 45 minutes per session, and will require you to repeat the same scan session five times over a period of a few months. You *will not* be compensated for your time. *The University of Nevada, Las Vegas may not provide compensation or*



UNLV
UNIVERSITY OF NEVADA LAS VEGAS
INFORMED CONSENT
Department of Health Physics



TITLE OF STUDY: Investigation of the Reproducibility of Functional Magnetic Resonance Imaging and Diffusion Tensor Imaging.

INVESTIGATOR(S): Jeremy Mangum, Phillip Patton

CONTACT PHONE NUMBER: 702-895-3555 (Phillip Patton), 702-453-4393 (Jeremy Mangum)

free medical care for an unanticipated injury sustained as a result of participating in this research study.

Contact Information

If you have any questions or concerns about the study, you may contact **Jeremy Mangum** at (702) 453-4393. For questions regarding the rights of research subjects, any complaints or comments regarding the manner in which the study is being conducted you may contact **the UNLV Office for the Protection of Research Subjects** at 702-895-2794.

Voluntary Participation

Your participation in this study is voluntary. You may refuse to participate in this study or in any part of this study. You may withdraw at any time without prejudice to your relations with the university. You are encouraged to ask questions about this study at the beginning or any time during the research study.

Confidentiality

All information gathered in this study will be kept completely confidential. No reference will be made in written or oral materials that could link you to this study. All records will be stored in a locked facility at UNLV for at least 3 years after completion of the study. After the storage time the information gathered will be shredded and disposed of appropriately.

Participant Consent:

I have read the above information and agree to participate in this study. I am at least 18 years of age. A copy of this form has been given to me.

Signature of Participant

Date

Participant Name (Please Print)

Participant Note: Please do not sign this document if the Approval Stamp is missing or is expired.



Biomedical IRB – Expedited Review Approval Notice



NOTICE TO ALL RESEARCHERS:

Please be aware that a protocol violation (e.g., failure to submit a modification for any change) of an IRB approved protocol may result in mandatory remedial education, additional audits, re-consenting subjects, researcher probation suspension of any research protocol at issue, suspension of additional existing research protocols, invalidation of all research conducted under the research protocol at issue, and further appropriate consequences as determined by the IRB and the Institutional Officer.

DATE: May 4, 2007
TO: Dr. Phillip Patton, Health Physics
FROM: Office for the Protection of Research Subjects
RE: Notification of IRB Action by Dr. John Mercer, Chair *omice*
Protocol Title: **Investigation of the Reproducibility of Functional Magnetic Resonance Imaging and Diffusion Tensor Imaging**
Protocol #: 0703-2287

This memorandum is notification that the project referenced above has been reviewed by the UNLV Biomedical Institutional Review Board (IRB) as indicated in regulatory statutes 45 CFR 46. The protocol has been reviewed and approved.

The protocol is approved for a period of one year from the date of IRB approval. The expiration date of this protocol is May 2, 2008. Work on the project may begin as soon as you receive written notification from the Office for the Protection of Research Subjects (OPRS).

PLEASE NOTE:

Attached to this approval notice is the **official Informed Consent/Assent (IC/IA) Form** for this study. The IC/IA contains an official approval stamp. Only copies of this official IC/IA form may be used when obtaining consent. Please keep the original for your records.

Should there be *any* change to the protocol, it will be necessary to submit a **Modification Form** through OPRS. No changes may be made to the existing protocol until modifications have been approved by the IRB.

Should the use of human subjects described in this protocol continue beyond May 2, 2008 it would be necessary to submit a **Continuing Review Request Form** 60 days before the expiration date.

If you have questions or require any assistance, please contact the Office for the Protection of Research Subjects at OPRSHumanSubjects@unlv.edu or call 895-2794.

Office for the Protection of Research Subjects
4505 Maryland Parkway • Box 451047 • Las Vegas, Nevada 89154-1047
(702) 895-2794 • FAX: (702) 895-0805



Brenda Durosinmi, MPA, CIP, CIM -Director
Office for the Protection of Research Subjects
University of Nevada Las Vegas
4505 Maryland Parkway Box 451047
Las Vegas, NV 89154-1047

Subject: Letter of Authorization to Conduct Research at Nevada Imaging Centers.

Dear Ms. Durosinmi:

This letter will serve as authorization for the UNLV researcher/research team, Phillip W Patton, PhD to conduct the research project entitled, Investigation of the Reproducibility of Functional Magnetic Resonance Imaging and Diffusion Tensor Imaging at Spring Valley Nevada Imaging Centers located at 5495 S. Rainbow Blvd. The research project has been reviewed by the appropriate facility administrative entity. Our legal advisor has also reviewed the project. We duly accept liability presented in the research project. The research may be implemented at the facility when the research project has received approval from the UNLV Institutional Review Board.

If we have any concerns or need additional information, the project researcher will be contacted and/or the UNLV Office for the Protection of Research Subjects.

Sincerely,

10/05/2006

Authorized Facility Representative Signature

Date

William W. Orrison Jr., M.D.
Print Representative Name and Title

Appendix D: Permission to Use Images

From: Glowniak, Jerry <jglownia@med.wayne.edu>
To: aroadnottaken@aol.com <aroadnottaken@aol.com>
Subject: RE: Permission to use image
Date: Sat, Dec 12, 2009 8:21 pm

Hi, Jeremy

Sorry for the late reply. It is okay to use the image, but please note that this is a modified Frank Netter illustration as noted on the bottom of the image on the right. It should be noted that the entire program is my creation. Dr. Zak is a neuroradiologist who I listed as an author since I needed his permission to use the research MRI scanner in the research area to obtain the MRI images. I see that you are a CNMT. I am board certified by the ABNM in nuclear medicine. Your research sounds interesting. Please let me know how your thesis is going. I would like very much to know what road it is that hasn't been taken.

Sincerely,
Jerry Glowniak, MD
Chief, Department of Radiology
Detroit Receiving Hospital
Detroit Medical Center/Wayne State University

From: aroadnottaken@aol.com [aroadnottaken@aol.com]
Sent: Saturday, October 31, 2009 5:55 PM
To: Glowniak, Jerry
Subject: Permission to use image

Dr. Glowniak,

My name is Jeremy Mangum from Las Vegas, NV. I am currently writing a Master's thesis on Olfactory response with fMRI at the University of Nevada Las Vegas. I came across your "Limbic System" website and liked the image you placed on the main page. I would like your permission to use this image in my thesis when I discuss the limbic system. I will, of course site your name and the name of your partner as mentioned on the webpage, Dr. Inad Zak. Thank you for your help with this, and please continue doing a great job. I appreciate the resources you've made available.

Yours,
Jeremy Mangum BS, CNMT, PET
aroadnottaken@aol.com

VITA

Graduate College
University of Nevada, Las Vegas

Jeremy Mangum

Degree:

Bachelor of Science, Nuclear Medicine, 2004
University of Nevada, Las Vegas

Special Honors and Awards:

Mitzi Hughes Alumni Scholarship
Golden Key National Honor Society
Society of Collegiate Scholars

Publications:

Supplement to Health Physics The Radiation Safety Journal, Abstract for National HPS Conference oral presentation, "Investigation of the Reproducibility of Functional Magnetic Resonance Imaging and Diffusion Tensor Imaging". Vol. 93, No. 1, pg. S43. July 2007.

Supplement to Health Physics The Radiation Safety Journal, Abstract for National HPS Conference poster presentation, "Comparison Between Region of Interest Selection Techniques Used in Diffusion Tensor Imaging Applied to the Corpus Callosum". Vol. 93, No. 1, p. S17. July 2007.

Thesis Title:

Development of a Functional MRI Olfactory Protocol

Thesis Examination Committee:

Chairperson, Phillip Patton, Ph. D.
Committee Member, Steen Madsen, Ph. D.
Committee Member, Ralf Sudowe, Ph. D.
Graduate Faculty Representative, Merrill Landers, DPT